AD NUMBER

AD845867

NEW LIMITATION CHANGE

TO

Approved for public release, distribution unlimited

FROM

Distribution authorized to U.S. Gov't. agencies and their contractors; Foreign Government Information; 01 DEC 1986. Other requests shall be referred to Central US Registry, 2530 Crystal Dr., Arlington, VA 22202.

AUTHORITY

SACLANTCEN ltr, 8 Jul 1970

Technical Report No. 129

SACLANT ASW
RESEARCH CENTRE

THE SUB-BOTTOM STRUCTURE OF THE GULF OF LA SPEZIA

by

L.R. BRESLAU and H. EDGERTON

1 DECEMBER 1968

NATO
VIALE SAN BARTOLOMEO, 400
I-19026-LA SPEZIA, ITALY

This document is released to a NATO Government at the direction of the SACLANTCEN subject to the following conditions:

1. The recipient NATO Government agrees to use its best endeavours to ensure that the information herein disclosed, whether or not it bears a security classification, is not dealt with in any manner (a) contrary to the intent of the provisions of the Charter of the Centre, or (b) prejudicial to the rights of the owner thereof to obtain patent, copyright, or other like statutory protection therefor.

2. If the technical information was originally released to the Centre by a NATO Government subject to restrictions clearly marked on this document the recipient NATO Government agrees to use its best endeavours to abide by the terms of the restrictions so imposed by the releasing Government.

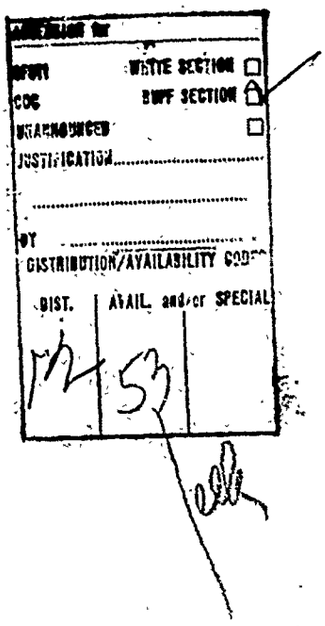

(14) TR-129

NATO UNCLASSIFIED

(9) TECHNICAL REPORT NO. 129

SACLANT ASW RESEARCH CENTRE
Viale San Bartolomeo 400
I 19026 - La Spezia, Italy

(6) THE SUB-BOTTOM STRUCTURE OF THE GULF OF LA SPEZIA.

(10) By

L.R. Breslau, H. Edgerton

(11) 1 Dec[redacted]68

(12) 89p.

APPROVED FOR DISTRIBUTION

Ir. M.W. van Batenburg
Director

NATO UNCLASSIFIED

312 950

elk

TABLE OF CONTENTS

FIGURES

TABLE OF CONTENTS (Cont'd)

APPENDIX A

THE SUB-BOTTOM STRUCTURE OF THE GULF OF LA SPEZIA

By

L.R. Breslau, H. Edgerton

ABSTRACT

The sub-bottom structure of the Gulf of La Spezia, Italy, has been investigated by continuous seismic profiling and sediment coring. The seismic profiles were used to develop contour plots of sub-bottom layers, which were identified from the core measurements.

The seismic profiles indicated a buried barrier bar extending across the Gulf, delineated by a rise in the terminal layer from more than 15 metres below the sea floor to less than 3 metres. Acoustically-opaque, dome-shaped features ("light domes") flank the barrier-bar. An acoustically-transparent layer ("shadow layer") hugs the terminal layer at the upper section of the barrier bar. Two intermediate-depth transparent layers ("main intermediate", and "deep intermediate" layers) are found landward of the barrier bar. The shallower of these ("main intermediate layer") terminates abruptly against either the barrier bar itself, or against the light domes fringing the bar's landward flank. A shallow-depth transparent layer ("shallow layer") is found distributed throughout the Gulf, apparently indpendent of the bar's influence. Acoustically-scattering patches ("dark patches") are found both landwards and seawards of the barrier bar, exhibiting a definite tendency to zone along depressions in the terminal layer.

Coring established that:

(1) The terminal seismic layer in the area of the barrier bar is related to a sand layer.

(2) The shadow seismic layer is related to a peat layer.

(3) The light domes are composed of coral.

(4) The dark patches are not noticeably related to a sediment type. Evidence suggests they are related to a volume distribution of scatterers.

(5) The main-intermediate and shallow seismic layers are not noticeably related to a sediment type, and these "layers" could therefore be the result of a random distribution of scatters on a plane or pseudo-plane.

INTRODUCTION

The existence of an extensive sub-bottom structure in the Gulf of La Spezia was observed by the authors in the autumn of 1964 during exploratory investigations with a continuous seismic profiler. This occurrence in shallow water close to a research centre afforded an opportunity to investigate the general problem of correlation of seismic discontinuities (manifest as sub-bottom acoustic layering) with sedimentalogic truth. Such research was therefore undertaken as part of SACLANTCEN's study of the acoustic reflectivity of the sea floor.

Preliminary results of the exploratory seismic investigation were presented in the autumn of 1964 [Ref. 1] to the Comité de Morphologie et Géologie Marine of the Commission pour l'Exploration de la Mer Méditerranée. Subsequent analysis of the profiles obtained during the exploratory seismic survey disclosed that the accuracy of the navigational positioning employed was inadequate to permit detailed contouring of the seismic layers, and another seismic survey was made in the autumn of 1965.

Thirteen sediment cores were obtained during 1965 and 1966, using the SACLANTCEN research vessel (MARIA PAOLINA) when opportunities occurred during arrivals and departures from La Spezia and during the test of coring equipment by the SACLANTCEN Oceanography Group. In addition, two electrical-resistivity sediment probings were made in early 1967 during tests of prototype equipment developed by the SACLANTCEN Oceanography Group.

This paper represents a final report on the seismic and sedimentalogic data collected.

1. GEOLOGIC SETTING

The Gulf of La Spezia [Fig. 1] is about 75 km southeast of Genoa. It is a remarkable instance of a deep landlocked gulf with no significant river flowing into it. It has a maximum land-sheltered length of about 7 km, an average width of 4.5 km, and a minimum width of 2.8 km between Point Pezzino and San Bartolomeo. The mouth of the gulf faces the sea toward the southeast. The gulf is now sheltered from the sea by a rock breakwater (constructed during 1870-1880), which runs approximately SW-NE from Point Santa Maria to Point Santa Teresa.

The gulf is ringed on its land perimeter by mountains of the Alpi Apuane [Ref. 2], a detached chain of the Tuscan Apennines. The western and eastern promontories consist of semi-parallel folds of mesozoic and younger rock [Ref. 2]: an overturned anticline on the west and a normal anticline on the east. The gulf is therefore basically a tectonic feature generated in response to deep-seated thrusting forces directed from southwest to northeast. This tectonic structure was subsequently flooded to form the actual gulf.

In general, the land bordering the western side of the gulf has stronger relief than that bordering the eastern side [Ref. 4]. The western promontory includes Mount Santa Croce (543 m), Mount Coregna (502 m), and Mount Castellana (510 m); the eastern promontory includes Mount Canarbino (310 m), Mount Rocchetta (415 m), and Mount Murlo (360 m).

There is a small, low-relief, alluvial area on the northwest shore (where the city of La Spezia stands), and a considerably larger one on the northeast shore. A relief map of the environs of the Gulf of La Spezia is included in Fig. 1.

Depths in the gulf (with the exception of dredged areas) at present range mainly between 10 m and 15 m, with 12 m as a representative value for the inner gulf (the part sheltered by the rock breakwater). The sea floor of the inner gulf consists entirely of grey clay with virtually no bottom relief.

The earliest available bathymetry records were found on a French chart dated 1846 [Ref. 5]. Data from this chart have been used to draw the 5, 10, 11, 12 and 13 metre contours shown on Fig. 1. It is interesting to note that a comparison between this bathymetry and present-day bathymetry of undredged areas [Ref. 6] has shown that shoaling of the inner gulf during the last 125 years has, on the average, either not occurred or been less than half a metre. In addition, for most areas the sediment notations on the old French chart ("vase grise") are the same as those in the present chart ("mud"). Apparently, the breakwater has not substantially altered either the bathymetry or the sediment type in the inner gulf.

Depths in the gulf (with the exception of dredged areas) at present range mainly between 10 m and 15 m, with 12 m as a representative value for the inner gulf (the part sheltered by the rock breakwater). The sea floor of the inner gulf consists entirely of grey clay with virtually no bottom relief.

The earliest available bathymetry records were found on a French chart dated 1846 [Ref. 5]. Data from this chart have been used to draw the 5, 10, 11, 12 and 13 metre contours shown on Fig. 1. It is interesting to note that a comparison between this bathymetry and present-day bathymetry of undredged areas [Ref. 6] has shown that shoaling of the inner gulf during the last 125 years has, on the average, either not occurred or been less than half a metre. In addition, for most areas the sediment notations on the old French chart ("vase grise") are the same as those in the present chart ("mud"). Apparently, the breakwater has not substantially altered either the bathymetry or the sediment type in the inner gulf.

2. SEISMIC INVESTIGATION

2.1 Method

Two separate surveys were made with continuous seismic profilers. The first exploratory investigation was made with a first-run production model of a continuous seismic profiler (the "Mud Profiler") installed on the SACLANTCEN workboat. Navigational position-fixing was by occasional optical bearings of land objects and steering was by compass course. Seismic records of excellent quality were obtained but the navigation proved inadequate for detailed contouring of the seismic layers.

The second seismic survey was made with an early engineering prototype of the"Mud Penetrator" (described below) installed on a small motorboat. Navigation was by steering on a fixed landmark and position fixing was by horizontal sextant angles on land objects. The seismic records obtained were usable for analysis but did not approach the quality of those obtained during the first survey.

Figure 2a shows the cruise tracks for the first survey and Fig. 2b those for the second survey. The solid lines represent cruise tracks made with navigation as described above. The optical bearings taken on the first survey were usually at 5 minute intervals, and the horizontal sextant angle readings on the second survey were usually at 2 or 3 minute intervals. A real-time navigational plot was kept during the second survey so that gross navigational errors would be immediately apparent. The dashed line in Fig. 2a represents a track made when navigating solely by shore line observation and distance estimation.

The "Mud Penetrator" seismic profiler [Refs. 7, 8, 9, 14, 15] is a commercially-available instrument that electronically generates an acoustic pulse in the water and records the arrival times of the acoustic echoes from the bottom and sub-bottom on an analogue correlation recorder. Echoes from acoustic discontinuities are synthesized by the correlation recorder so that a graph of the bathymetry and sub-bottom structure along a profile is obtained directly. The principal features of the "Mud Penetrator" that give it the capacity to penetrate the sea floor and resolve fine structure are its high peak power output (about 105 dB//1 dyne/cm^2), short pulse length (about 0.1 ms), and high repetition rate (10 or 20 pulse/s).

The equipment is in three parts: (1) a recorder/driver console; (2) a transducer; (3) a gasoline-powered electric generator. The recorder/driver console generates the acoustic pulse and records its echo. The transducer, which has a beam width of 30^{o}, is used for both transmitting and receiving the acoustic pulse. It uses a piezoelectric crystal for energy conversion, and must be submerged during operation.

This equipment was installed on the 65 ft SACLANTCEN workboat, the transducer being housed in a streamlined "fish" towed alongside the boat at a depth of approximately two metres. The survey was conducted at speeds of 2 or 3 knots.

2.2. Results

The seismic results are presented in the form of annotated seismic profiles, and of contour and areal distribution charts of seismic features compiled from seismic profiles. The high-quality seismic records obtained during the first survey are used for profile display and specification of sub-bottom features. The seismic records obtained during the second survey, when position fixing was more accurate, were used to develop the contour and areal distribution charts.

Some fundamentals concerning the interpretation of continuous seismic profiler records should be mentioned. Taken by itself, this type of seismic information is ambiguous. An indication of sub-bottom structure on the seismic record can be accepted as proof of the existence of sub-bottom structure, but the absence of an indication of sub-bottom structure on the seismic record does not necessarily mean that sub-bottom structure does not exist. This is because the reception of a signal from a sediment interface depends on the magnitude of the acoustic reflection from the interface as well as on the acoustic attenuation in the overlying sediment layer. Therefore, sub-bottom structure might actually be present and yet not record, because of masking by a highly-attenuating sediment cover.

The interpretation of magnitudes of seismic reflections must not only take account of attenuation in overlying sediment cover, but also of the depth-dependent propagation loss in the water column, and of various gain settings on the seismic apparatus itself. In addition, the dynamic range in the recording paper used with the seismic system is only 20 dB under the best laboratory conditions, and probably considerably less when used at sea. Therefore, the reflecting strengths of the seismic layers observed on the record can only be discussed in very qualitative terms.

Figure 3 gives the locations of the selected seismic profiles presented in Figs. 4-10. It should be noted that the horizontal axis of the latter is the elapsed time during a profiling run and that no information on geographical direction is inherently contained in the profiles. The geographical direction of the horizontal axis is indicated both by the arrows on the cruise tracks in Fig. 3 and by the subscripts to the individual profiles' letter identifiers in Figs. 3-10.

Printed annotations have been added to the otherwise unaltered seismic profiles presented in Figs. 4-10. These annotations, based on a descriptive rather than generic system, serve to point out the significant sub-bottom seismic features observed in the profiles. The following is a list and description of these features:

Deep Layer: Good examples are found in Profile N [Fig. 6] and Profile a [Fig. 8]. This layer is a good reflector and poor transmitter of acoustic energy. It is the terminal reflector (deepest layer that has been reached with the particular seismic apparatus used) and appears on all the profiles. It is observed at depths ranging from 8 m in Profile A [Fig. 4] to 28 m in Profile M [Fig. 5]. Morphologically, it seems to represent a composite feature resulting from the superposition of a raised cross-gulf barrier bar, Profile B [Fig. 9], on a seaward-dipping basement. The landward flank of the barrier bar is considerably steeper than the seaward flank, and the bar's crest shoals to less than 3 m below the sea floor.

Light Dome: Good examples are found in Profile E [Fig. 4], Profile M [Fig. 5], and Profile Q [Fig. 6]. This feature is a good reflector and a very poor transmitter of acoustic energy. In fact, it is almost totally opaque acoustically. The light appearance on the seismic record results from the absence of any acoustic energy return after the first-arrival echo from the upper surface of the light dome. They are commonly found on the inner and outer flanks of the cross-gulf barrier bar [Profile M (Fig. 5) and Profile Q (Fig. 6) respectively], and in a zone in the northeast section of the inner gulf (Profile E, Fig. 4). The upper surface of the light domes is observed at depths ranging from 10 m (Profile C, Fig. 4) to 16 m (Profile e, Fig. 9). This upper surface is usually found touching or slightly below the shallow layer (Profiles O and Q, Fig. 6), but it may also be found slightly above this layer (Profile P, Fig. 6) and considerably below it (Profile e, Fig. 9).

Dark Patch: Good examples are found in Profiles J, K, L and M [Fig. 5], Profiles N and O [Fig. 6], and Profiles b and c [Fig. 9]. This feature is a partially transparent diffuse reflector. The echo return is stretched out as if the acoustic wave passed through a concentrated assemblage of small but good reflectors. Dark patches most prominently occur at depressions in the deep layer (Profiles J and K, Fig. 5). They also occur, however, in a zone at the middle western part of the inner gulf [Profile M, west end (Fig. 5), Profiles N and O (Fig. 6)], and here they are not obviously related to a deep layer depression. The upper surface of the dark patches is found between depths of 10 m (Profile C, Fig. 4) and 22.5 m (Profile W, Fig. 7). A representative depth in the major deep-layer depression landward of the cross-gulf barrier is about 20 m (Profile K, Fig. 5); in the middle western zone it is about 15 m [Profile M, west end (Fig. 5)]. All these depths are approximate because it is rather difficult to specify the depths of the upper surfaces of the dark patches owing to their diffuse and irregular character.

Main Intermediate Layer: Good examples are found in Profiles J, K, L and M [Fig. 5]. This layer is both a good reflector and a good transmitter of acoustic energy. The echo return from this layer is strong enough to record well on the seismic record, and yet there is no evidence that the presence of this layer obscures any underlying features. It is interesting to note that there is a tendency for echo strength to increase with the depth of this layer (Profile b, Fig. 9). It is only found landwards of the cross-gulf barrier-bar; its southeastern border either terminates against the barrier bar [Profiles J, K, L and M (Fig. 5), and Profile c (Fig. 9)], or against the light domes on the inner flank of the barrier bar [Profiles X, Y Z and a (Fig. 8), Profile b (Fig. 9)]. This layer is found at depths between 12 m (Profile H, Fig. 4) and 27 m (Profile L, Fig. 5). Though it is not conformal to the surface of the deep layer, slight depressions in it do occur over areas of depression in the deep layer [Profile X, mid-profile (Fig. 8)].

Deep Intermediate Layer: Good examples are found in Profile M [Fig. 5] and Profiles U, V and W [Fig. 7]. This layer appears to be acoustically similar to the main intermediate layer. It is found within the area of existence of the main intermediate layer, but is more restricted in area. It does not impinge against the light domes or cross-channel barrier-bar, but rather pinches out towards the southeast. It is found at depths between 16 m (Profile H, Fig. 4) and 20 m (Profile K, Fig. 5). Though it is not conformal to the surface of the deep layer, there is a correlation between depressions in both surfaces (Profile K, Fig. 5), which is similar but somewhat stronger than that observed between the main intermediate layer and the deep layer.

Shallow Layer: Good examples are found in Profiles N, O, P and Q [Fig. 6]. This layer is a weak reflector and excellent transmitter of acoustic energy. It is almost transparent acoustically. It is observed on most of the profiles and appears at about 2 to 3 m below the present-day sea floor. It probably exists even where not seen on the record, but is lost in the echo return from the sea floor. Its weak echo strength and conformality with the sea floor topography led to suspicion that it represented an extraneous reflection from the boat. This suspicion was dispelled by an experiment in which the seismic transducer was lowered to depths of up to 10 m below the boat, during which time the shallow layer remained at a constant depth relative to the sea floor trace on the seismic record.

Multiple Shallow Layers: Good examples are found in the eastern sections of Profiles N, O, P and Q [Fig. 6]. Two layers, of similar acoustical character to the shallow layer, are observed within a depth zone about 1 m thick above the shallow layer in the southeastern section of the inner gulf.

Shadow Layer: Good examples are found in Profiles b, c, d, e and f [Fig. 9]. This layer is a good reflector and a good transmitter of acoustic energy. It is confined to a zone near the crest of the cross-gulf barrier-bar, where it is found associated with, and less than 1 m shallower than, the deeper layer. Its name originates from the fact that it has the appearance on the seismic record of a shadow on top of the deep layer.

Buried Channels: Good examples are found in Profiles C, D, E and F [Fig. 4]. This feature appears on the seismic record in the form of a trough-shaped depression in the deep layer. These depressions are up to 3 m deep and usually contain small-scale, semi-conformal layering within them. The zone of occurrence of this feature is limited to the area landward of the cross-gulf barrier-bar.

Upper and Lower Discontinuous Layers: Good examples are found in Profiles J, K, L and M [Fig. 5]. These layers are characterized principally by their disjointed or discontinuous appearance. The reflecting fragments themselves are good acoustic reflectors, which sometimes display a tendency toward crescentic shapes. The layers are observed landward of the cross-channel barrier-bar. Where the discontinuous layers and deep intermediate layer are observed concurrently, the upper discontinuous layer is found about 1.5 m above, and the lower discontinuous layer about 1 m below, the deep intermediate layer.

Second Bottom: This is not a seismic layer but rather a manifestation of a multiple reflection of the echo from the sea floor. The acoustic path is ship to sea-floor to sea-surface to sea-floor to ship.

Contours and area distributions of the deep layer, main intermediate layer, deep intermediate layer, shallow layer, multiple shallow layers, light domes, and dark patches are presented in Figs. 11-13. These charts represent a detailed analysis of all the seismic records obtained during the second seismic survey [Fig. 2b]. Depths are referenced to the sea surface.

The deep layer [Fig. 11] represents the terminal layer (deepest layer reachable with the particular seismic apparatus used) in the Gulf of La Spezia. Two separate morphological features are evident: a raised cross-gulf barrier-bar (gently contoured depositional feature) and a deeply eroded older surface upon which the barrier bar is superimposed. There is a lapse in the contouring of the landward flank of the cross-gulf barrier-bar because the presence of light domes obscured the deep layer.

The main intermediate layer was observed in the area shown in Fig. 12a, which also indicates the depth contours of the layer. The deep intermediate layer is shown in a similar fashion in Fig. 12b. As seen in Fig. 12d, the area of existence of the deep intermediate layer is totally included within the area of existence of the main intermediate layer.

The shallow layer was definitely observed in the area shown in Fig. 12c. The dash-line bordered addition to this area towards the northwest indicates its probable existence (marginal indication on seismic record). The multiple shallow layers were observed south of the border indicated by the dotted line and within the area of existence of the shallow layer.

The areas of intermediate and shallow layers recorded in Figs. 12a, b, and c are shown together in the combined chart of Fig. 12d.

The areal distribution of the light domes and dark patches is shown in Fig. 13. Clearly, both of these features have a strong tendency towards zonal rather than random distribution. The light domes (represented by solid line segments) occur along a narrow band on the inner and outer flanks of the cross-gulf barrier-bar, and within a broader, bank-like zone in the northeast section of the inner gulf. The dark patches (represented by dashed-line segments) occupy three general zones: a northerly-tending elongated zone landward of the cross-gulf barrier-bar, a zone in the western section just landward of the barrier-bar, and a small (possibly elongated) zone just seaward of the barrier bar.

3. SEDIMENTALOGIC INVESTIGATION

3.1 Sampling Methods

The continuous seismic profiling investigation provided information about the existence of sub-bottom layers. A sedimentalogic investigation was made to provide information about the actual nature of these sub-bottom layers. This sedimentalogic investigation consisted of the acquisition and analysis of 7 surficial sediment dredge hauls, 6 narrow-barrel sediment corings, and 13 wide-barrel sediment corings. The dredge hauls and narrow-barrel sediment corings were made within a few months after the exploratory seismic investigation. While some questions were answered, more were raised, and this phase of the sedimentalogic investigation should be considered exploratory. The detailed sedimentary investigation utilizing the wide-barrel corer was made during a two-year period whenever the SACLANTCEN research vessel was available, and as sediment sampling and analysis equipment was developed by the SACLANTCEN Oceanography Group.

A clamshell grab dredge was used to obtain undisturbed surficial sediment samples. A sediment sample for subsequent water-content analysis was obtained by pressing a tin can into an undisturbed surface section of the dredge haul and then transferring the contents of the can to a pre-weighed bottle.

The narrow-barrel sediment corer (called the "bomb" corer) was built by attaching three metres of 5 cm bore pipe to the nose of a standard ASW bomb filled with concrete. A clear plastic tube was fitted inside this pipe. In operation, the bomb corer fell freely from the sea surface and the pipe was driven into the sea floor. The corer was then retrieved, the clear plastic liner containing the sediment core removed, and the retained sediment examined by sight and touch.

The natures of the surficial sediment cover, deep layer, shadow layer, and light domes were established by these means. Unfortunately, the nature of the shallow layer proved elusive, and the intermediate layers and dark patches lay beyond the penetration depth range of the bomb corer. Therefore, the SACLANTCEN wide-barrel piston corer (then under development) was used to sample these layers, which were then subjected to detailed mass-physical sediment analysis to determine their nature.

The SACLANTCEN wide-barrel piston corer [Ref. 12] is a long corer with a watertight core-catcher and electrical trigger release system. It is designed specifically for obtaining undisturbed sediment samples for mass-physical analysis. When used with a 12 m coring barrel its total length is 15 m and total weight 1000 kg. A 12 cm diameter plastic liner fits inside the core barrel and retains the sediment section.

This corer was used from the SACLANTCEN Research Vessel to obtain 13 sediment cores. These cores were taken by gravity rather than by using the piston, because the hydrostatic head available was insufficient for piston coring. The depth that the core barrel penetrated into the sea floor was noted by sediment markings on the outside of the core barrel. This figure was recorded for later use in applying a stretch factor to the sediment sections recovered in the liner. The sediment-filled liners were analyzed in the laboratory.

The geographical locations of the surface sediment dredge hauls and wide-barrel core stations are indicated in Fig. 14 by symbols S1 to S7, and C1 to C13, respectively. These geographical locations are also tabulated (Table A.1) in Appendix A to this report. The "bomb" cores were taken near the crest of the cross-channel barrier-bar and over a light dome on the landward flank of the barrier-bar. Precise geographical locations were not obtained.

3.2 Analysis

3.2.1 Methods

Three methods of sediment analysis were used. These, in ascending order of complexity and difficulty, are as follows: visual analysis, water content analysis, and sound speed analysis. The sediments were subjected to one or more of these analyses.

The visual analysis can be made rapidly in the field. The water content analysis certainly requires more effort than the visual analysis, but is still easy to perform, since all that is required is one oven-drying and two weight measurements. The sound speed analysis is tedious to make, requires complex equipment, and the measurements are liable to error unless the operators are very careful.

3.2.2 Visual Analysis

The visual analysis consists simply of visual and manual examination of the sediment. This is sufficient to determine the sediment type, of which the following can be indentified by an experienced investigator: clay, clay and silt, silt, sand, gravel, coral, peat, and shell material.

3.2.3 Water Content Analysis

From the direct measurement of the water content of a sediment, reasonably valid assumptions can be used to deduce other mass-physical quantities [Refs. 10, 11]. Water content is defined in soil mechanics as the ratio of the weight of water in a sediment to the weight of solid sediment matter. This ratio was measured direct by finding the wet (natural state) and dry (oven-dried at $105^{\circ}C$ for 24 hours) weights of the sediment.

Porosity is defined as the volume fraction of the sediment occupied by sea water. It was computed from the water content measurements using the formula:

$$\varphi = \rho_{particles} \times W / \left[\rho_{particles} \times (W + 1) \right]$$

where φ is the porosity, $\rho_{particles}$ the average density of the solid sediment particles, and W the measured water content. A value of 2.67 was assumed for the average density of the solid sediment particles. This assumption rests on the empirical observation that the range of specific gravities of minerals commonly occuring in natural marine sediments is slight and that 2.67 is a good representative value. Density is considered as the bulk density of the sediment. It can be computed according to the formula:

$$\rho_{bulk} = \rho_{water} \times \varphi + \rho_{particles} \times (1 - \varphi)$$

where

ρ_{bulk} is the density of the sediment,

ρ_{water} is the density of sea water,

$\rho_{particles}$ is the average density of the solid sediment particles, and

φ the computed porosity.

A value of 1.02 was assumed for the density of sea water at the bottom of the Gulf of La Spezia.

3.2.4. Sound Speed Analysis

Sound speed analysis consists of a direct measurement of the transit time of an acoustic pulse between two probes implaced in the sediment. The probes are placed radially to the axis of a sediment core and contact the sediment through holes drilled in the plastic liner. The actual measurement is made

by aligning the leading edge of the transmitted and received pulses by the injection of a calibrated time delay into the system. Naturally, the distance between the probes is known. This analysis technique has been described in detail by Kermabon [Ref. 17]. The sound speed analysis was performed by the SACLANTCEN Oceanography Group.

3.3 Results

The surface sediment samples were subjected to a water content analysis. The measured water content, computed porosity, and computed density are presented in Table 1.

TABLE 1

MASS PROPERTIES OF SURFACE SEDIMENT SAMPLES

Surface Sediment Sample	Water Content (Ratio)	Computed Porosity (Percent)	Computed Density g/cm^3
S1	1.347	78.2	1.38
S2	1.086	74.4	1.44
S3	0.974	72.2	1.48
S4	0.979	72.3	1.48
S5	0.881	70.2	1.51
S6	1.344	78.2	1.38
S7	1.465	79.6	1.36

From these measurements, inspection of other dredge hauls taken at random locations in the gulf, and discussions with Italian Navy divers, it is concluded that the inner gulf has a high-porosity, fine-grained sediment cover; this, incidentally, closely resembles the sediment cover commonly found in the deep sea.

The sedimentalogic results obtained from the cores taken with the wide-barrel corer are shown graphically in Figs. 15-21, and listed more fully in Table A.2 of Appendix A. The distance shown in the graphs is the stretched distance, which is the original distance along the sediment section multiplied by the stretch factor for that core. The latter is determined by "stretching" the actual sediment section recovered to the length of known core barrel penetration. A linear sediment recovery rate is assumed.

Sediment cores C2, C4 and C11 were subjected to visual, water content, and sound speed analyses; the results are presented in Figs. 15, 16 and 17 respectively. Acoustic impedance was calculated by taking the product of the sediment density and the sound speed. The sampling interval for these cores was 10 cm of the original distance along the length of the sediment core. The sedimentalogic results presented in the figures are sediment type, porosity, density, sound speed, and acoustic impedance. The sound speed measurement (and therefore also the acoustic impedance calculation) of Core C4 [Fig. 16] is suspect, both because of the way it appears on the graph and because of known instrumentation difficulties.

Sediment Cores C1, C3, C8, C10, C12 and C13 were subjected to visual and water content analyses. The sediment types, porosities, and densities of these six cores are presented in Figs. 18-20. The sampling interval was 10 cm (original length) for C8 and 50 cm (original length) for the other five cores. Duplicate samples were taken on these five cores in order to test the precision of the water content analysis. The spread in these measurements is too small to be resolved in the graphs, but this information is contained in Table A.2 of Appendix A.

Sediment Cores C5, C6, C7 and C9 were examined visually. Sediment Core C7 was found to contain substantial amounts of coral (Madreporaria Perforata, a white Dendritic Branching Coral), and therefore the weight of coral in each 10 cm (original length) segment was also determined. The sedimentalogic results, consisting of sediment type for all the cores and coral content for Core C7, are presented in Fig. 21.

The sediment cores obtained during the exploratory investigation with the bomb corer were visually analyzed. These results agreed with those later obtained from the investigation with the wide-barrel corer. A bomb core station taken over a light dome showed the presence of coral. Bomb core stations taken near the crest of the cross-channel barrier-bar showed the sediment section to be clay overlying peat overlying sand. The shallow layer was penetrated but could not be identified in the core.

CONCLUSIONS

The seismic results contained separately in Figs. 11 and 13 are combined in Fig. 22, to give a composite display of deep-layer contours, light domes, dark patches, and sediment sites. Those contained separately in Figs. 12 and 13 are combined in Fig. 23 to give a composite display of intermediate and shallow layer contours, light domes, dark patches and sediment sites.

From the contours of the deep layer shown in Fig. 22 it is seen that the light domes tend to be located along the inner and outer flanks of the raised cross-gulf barrier-bar and that the dark patches tend to concentrate in the deep depressions in the basement. Figure 23 shows that the dark patches have no discernible relationship with the intermediate and shallow layers. The main intermediate layer terminates abruptly against the light domes at its southern boundary and blankets some of them toward its eastern boundary. The borders of the deep intermediate layer do not extend to the light domes.

The types and depths of seismic features recorded at the thirteen coring sites are presented in Table 2. The information in Figs. 22 and 23 has been used to specify the existence of seismic features and the depths to the seismic layers. The depths of the tops of the light domes and dark patches were derived from examination of seismic records at the appropriate core sites.

Seismic and sedimentalogic information for the coring sites are presented together in Table 3 in order to facilitate examination of the degree of correlation between them. The seismic information of Table 3 has been derived from data contained in

TABLE 2

SEISMIC FEATURES PRESENT AT SEDIMENT CORE SITES

Sediment Site	Seafloor (m)	Shallow Layer (m)	Main Intermediate Layer (m)	Deep Intermediate Layer (m)	Deep (Terminal) Layer (m)	Dark Patch Top (m)	Light Dome Top (m)
C1	11.6	14.0	----	----	15.0	----	----
C2, C3	11.8	14.5	----	----	19.6	----	----
C4, C5	11.9	14.6	----	----	20.5	----	----
C6	12.0	14.7	----	----	23.2	----	----
C7	11.7	14.0	----	----	?	----	14.5±.5
C8	12.6	----	19.0	----	25.5	----	----
C9	11.2	----	19.0	----	25.0	----	----
C10	10.6	----	17.1	21.1	27.8	24±1	----
C11	12.8	----	17.0	20.6	24.0	----	----
C12	12.6	----	16.5	----	28±	19±1	----
C13	12.1	----	----	----	28±	18±1	----

Table 2, with conversion of depth reference from sea surface to sea floor to make it compatible with the sedimentalogic information. The sedimentalogic information of Table 3 has been derived from the core data contained in Figs. 15 to 21. Only sediment type information is given in the table and it is necessary to refer to the figures for information on mass-physical properties of the sediments and the presence of various inclusions (shells, etc.) found in the cores.

Examination of Table 3 reveals the following information:

a. The deep layer (terminal layer) at the cross-gulf barrier-bar is related to a sand layer. Evidence is found in Cores C1, C2, C3, C4 and C5.

b. The shadow layer, discussed in the seismic analysis [Sect. 2.2] is related to a peat layer. Evidence is found in Core C1.

c. The light domes are composed of coral. Evidence is found in Core C7.

d. The shallow layer is not related to a layer consisting of a particular sediment type. This seismic layer was definitely penetrated by Cores C1, C2, C3, C4, C5 and C6, but no detectable variation in sediment type was observed in the cores.

e. The dark patches might be related to the presence of large amounts of shell material in the sediment. They are not noticeably related to a particular sediment type in the geologic sense of the word. Evidence is found in Core C13.

f. The main intermediate layer is not related to a layer consisting of a particular sediment type. This seismic layer was definitely penetrated by Cores C11 and C 12, and possibly penetrated by Core C9, but no variation in sediment type was detected in the cores.

TABLE 3

COMPARISON OF SEISMIC AND SEDIMENTALOGIC INFORMATION AT CORE SITES C1-C13

Sediment Site	Seismic Information — Features and their Depth Below Seafloor				Sedimentalogic Information		
	First Seismic Feature (Layer)	Second Seismic Feature (Layer)	Third Seismic Feature (Layer)	Fourth Seismic Feature (Layer)	Length of Sediment Section Received	Depth of Maximum Core Penetration	Sediment Type
C1	Shallow 2.4 m	Terminal 3.4 m	-	-	5.7 m	8.0 m	0m-3.0m Grey Clay 3.0m-3.6m Peat 3.6m-7.7m Sand 7.7m-8.0m Gravel
C2	Shallow 2.7 m	Terminal 7.8 m	-	-	3.65 m	5.5 m	0m-5.2m Grey Clay 5.2m-5.5m Sand
C3	Shallow 2.7 m	Terminal 7.8 m	-	-	3.45 m	6.0 m	0m-5.8m Grey Clay 5.8m-6.0m Sand
C4	Shallow 2.7 m	Terminal 8.6 m	-	-	4.2 m	7.0 m	0m-6.9m Grey Clay 6.9m-7.0m Sand
C5	Shallow 2.7 m	Terminal 8.6 m	-	-	4.7 m	7.1 m	0m-6.6m Grey Clay 6.6m-7.1m Sand
C6	Shallow 2.7 m	Terminal 11.2 m	-	-	4.5 m	7.2 m	0m-7.2m Grey Clay
C7	Shallow 2.3 m	Light Dome 2.8 ± .5 m	-	-	5.6 m	6.5 m	0m-3.7m Grey Clay 3.7m-6.5m Clay & Coral.
C8	Main Int. 6.4 m	Terminal 12.9 m	-	-	5.0 m	6.0 m	0m-6.0m Grey Clay
C9	Main Int. 7.8 m	Terminal 13.8 m	-	-	4.2 m	8.1 m	0m-8.1m Grey Clay

TABLE 3 (Cont'd)

COMPARISON OF SEISMIC AND SEDIMENTALOGIC INFORMATION AT CORE SITES C1-C13

Sediment Site	Seismic Information — Features and their Depth Below Seafloor				Sedimentalogic Information		
	First Seismic Feature (Layer)	Second Seismic Feature (Layer)	Third Seismic Feature (Layer)	Fourth Seismic Feature (Layer)	Length of Sediment Section Received	Depth of Maximum Core Penetration	Sediment Type
C10	Main Int. 6.5 m	Deep Int. 10.5 m	Dark Patch 13.4 ±1 m	Terminal 17.2 m	4.6 m	6.0 m	0m-5.0m Grey Clay
C11	Main Int. 4.2 m	Deep Int. 7.8 m	Terminal 11.2 m	-	4.45 m	7.5 m	0m-7.5m Grey Clay
C12	Main Int. 3.9 m	Dark Patch 6.4 ±1 m	Terminal 15.4 m	-	5.8 m	7.5 m	0m-7.5m Grey Clay
C13	Dark Patch 5.9 ±1 m	Terminal 15.9 m	-	-	7.5 m	8.0 m	0m-3.8m Lost 3.8m-8.0m Grey Clay (considerable shell material)

g. The deep intermediate layer was not penetrated by any of the cores.

h. A gravel layer exists below the sand layer at the cross-gulf barrier-bar, but this layer was undetected by the seismic system, owing to masking by the sand (terminal) layer.

Conclusions a to d above are additionally substantiated by the results obtained during the exploratory sedimentalogic investigations with the bomb corer. Conclusion c is reinforced by results obtained by the harbour dredgers, which reported the dredging of great quantities of hard coral formations together with mud:

"Nelle zone fangose si è osservata la presenza di formazioni coralligere costituite da una specie di corallo bianco poroso di notevole durezza che veniva dragato in quantità rilevante misto al fango",

("in the mud zones we observed coral formations made of a kind of very hard white porous coral, which was dredged in great quantity together with the mud"). (Private Communication, Agenzia Gastaldi, Naples, Italy).

Additional information bearing on the nature of the dark patches discussed in Conclusion e above can be found in the results of a test borehole taken for civil engineering purposes in the western part of the gulf. The location of the borehole site [Table A.3, Appendix A] is indicated as D1 on Figs. 22 and 23. This site is located over a dark patch whose top is 18 ± 1 m below sea level. The borehole sediment log indicates silty clay and clayey silt from the sea floor down to a depth of 28 m below sea level, where a sand layer is encountered. The annotations concerning inclusions are enlightening. At 15.5 m the log states "Argilla limosa grigia con tracce di torba e framm. di conchiglie", ("grey silty clay with traces of peat and shell fragments"). The next notation is

at 19.5 m, where the log states "limo argilloso con torba a grumi e diffusa e framm. di conchiglie", ("clayey silt with peat both in patches and diffused, and with shell fragments"). (Private communication, S.N.A.M. SA, Sondaggio 17 Seno di Panigaglia, Studio Technico Geom. Celctti, Milano).

Some test boreholes have been made in the area surrounding the gulf for engineering purposes. Their locations are contained in Table A.3 of App. A, and indicated in Figs. 22 and 23 as symbols D1 and D6. Sediment borehole D1 has already been discussed in connection with the dark patches. Boreholes D2-D6 contribute little, if any, information relating to identification of seismic features observed in the gulf. A brief résumé of their results is listed in Table A.4 of App. A.

The nature of the shallow and intermediate layers is not clearly established. Sediment Cores C1, C2, C3, C4, C5 and C6 certainly penetrated the shallow layer. It has already been stated that no relation could be established on the basis of sediment type (Conclusion d above). The water content analysis for Cores C1, C3, C2 and C4 [Figs. 15, 16 and 18] does not disclose any variation in porosity or density that can be related to this layer. Although Cores C1 and C3 were sampled at 50 cm intervals and represent only spot measurements, Cores C2 and C4 were sampled at 5 cm intervals and their sample spacing should have been adequate to resolve significant variations. The sound speed analysis for Core C2 [Fig. 15] does not disclose any variation in sound speed or acoustic impedance that can be related to the shallow layer. The sample interval for this analysis was 5 cm and significant variations should have been detected. The results of the sound speed analysis on Core C4 [Fig. 16] are considered suspect and discounted.

Sediment Cores C11 and C12 definitely penetrated the main intermediate layer, and Core C9 might have penetrated it. It has already been stated that no relation could be established on the basis of sediment type (Conclusion 6 above). The water

analyses for Cores C11 and C12 [Figs. 17 and 20] and the sound speed analysis for Core 11 do not disclose any significant variations. The sampling interval in Core C11 for both analyses was 5 cm, and significant variations should have beer resolved. A definite conclusion regarding the nature of the shallow and intermediate layers has not been reached, but the authors wish to present a hypothesis that they feel most probably represents the situation. This is that these layers are not layers in the sense of a sediment/sediment interface but simply represent a random distribution of acoustic scatterers (sediment patches, shells, peat, etc.) occupying a preferred horizon. Only very minor evidence exists to support this hypothesis: this is as follows: a 4 cm shell was noted in Core C4 [Fig. 16] at a depth of 2.6 m, shell fragments 1-3 cm long were noted in Core C6 [Fig. 21] at a depth of 2.7 m, and a 4 cm shell was noted in Core 11 [Fig. 17] at a depth of 3.8 m. This evidence is depreciated by the existence of other shells in these and other cores. The hypothesis has been arrived at by elimination of other possible explanations. There are only three possibilities: (a) the shallow and intermediate seismic layers are artificial and are caused by spurious acoustic reflection; (b) the layers are real and sedimentalogic evidence concerning their existence is contained in the cores; (c) the layers are real but the coring process did not adequately sample the phenomenon responsible for their existence.

The first possibility is discredited by the fact that another investigator [Ref. 19], using a different seismic system (50 kHz), noted the existence of these seismic layers. In addition, the present authors lowered the seismic transducer almost to the sea floor to make certain that the shallow layer was not caused by a spurious reflection from the boat. The overall appearance (abrupt termination against light domes) and geographical zoning of the intermediate layers attest to their geologic credibility.

The second possibility is discredited by the thoroughness of the core sampling and analysis. This is especially so with regard to the shallow layer. It is certain that at least five cores (C1-C5) penetrated this layer, because they sampled the underlying sand layer. If something responsible for the shallow layer was present in the cores, it should at least have been detected by the high-resolution water-content analysis, since porosity is probably the single most important mass physical characteristic of sea floor sediments for producing an acoustic impedance change, and the 5 cm sampling interval that was used is shorter than the wavelength of 12 kHz sound in the sediment. Additional information attesting to the vertical homogeneity of the sediment column above the sand layer in the area where the shallow layer is present, was the constancy of the electrical resistivity profile obtained during two sediment probings by the SACLANTCEN Oceanography Group during tests of prototype equipment [Ref. 20]. The third possibility, therefore, remains. Although there is no significant evidence to support it, there is also none to disprove it.

This third possibility — that the coring process did not adequately sample the phenomenon responsible for the seismic layering — would be exactly what could be expected if there was a random distribution of acoustic scatterers located on a plane or pseudo-plane. That this situation was responsible for the shallow and intermediate layers is seismically and geologically plausible. The existence of a "layer" on the record produced by a continuous seismic profiler indicates only that moderately repetitive echoes were received during a certain period of time from some reflecting points located both within the sensitivity zone of the sonic beam and at a constant or slowly-changing distance from the ship. Since the full angle beamwidth of the transducer sensitivity cone used was 30^{o}, it can readily be seen that the density of scatterers required to produce a "layer" is not large (one large scatterer per 5 m^2 when located on a plane 12 m from the ship).

From the geological standpoint, it is perfectly reasonable to expect the random distribution of scatterers on a plane or pseudo-plane to occur in nature. This could be caused by biogenic material, sediment patches, or primary sedimentary features such as burrows, mounds, or ripples [Ref. 17] located on a plane or pseudo-plane representing an ancient sea floor, and preserved in the stratigraphic column. In fact, this line of reasoning, coupled with the results of this controlled experiment in the Gulf of La Spezia, raises the question of the actual nature of the shallow seismic layering recently reported as common in many parts of the deep sea.

One rather unfortunate fact brought out in Table 3 is that the technique employed in this investigation to compare seismic and sedimentalogic information needs refinement if more detailed analysis is to be attempted. For example, while it is obvious that the sand layer found in Cores C1, C2, C3, C4 and C5 represents the terminal seismic layer (Conclusion a above), it is distressing to note that only Core C1 should have been deep enough to penetrate the terminal layer. A combination of factors probably contributed to this situation. Operational circumstances made it impossible to run the seismic and sedimentalogic phases of the investigation simultaneously; therefore some of the inconsistencies are probably attributable to positioning errors in sampling. In addition, limitations in navigational accuracy precluded relating the cores to single seismic profiles; thus the seismic information tabulated represents data that have been contoured and to some extent degraded in accuracy. Another problem is in the coring technique itself. The assumption of a linear sediment recovery rate is weak, although considered the best assumption in the absence of other information. Obviously, the sediment that first enters the core barrel encounters less resistance (with attendant higher recovery rate) than the sediment subsequently entering. A sediment corer that can continuously monitor

the sediment recovered, and record this as a function of penetration depth, needs to be developed.

The conclusions reached in the examination of Table 3 were based mainly on sediment sequence rather than sediment existence at a specified depth. This is sufficient to deal with relatively clear-cut cases such as sediment/sediment interfaces, but is not adequate to properly treat subtle cases, which might require detailed statistical analysis. The shallow and intermediate layers of the Gulf of La Spezia are considered to fall within the latter category.

A summary of the geology of the Gulf of La Spezia is presented in Figs. 24 and 25, the locations of the standard geologic sections in Fig. 24 being indicated on the map of sub-bottom geology in Fig. 25. In the latter map, the area surrounding the gulf was drawn from a map made over a century ago [Ref. 3] and represents the area as it was before man extensively altered the shoreline and river channels. The widths of lines indicating the rivers are representative of relative river size. Two springs that were once present in the area (one of them an underwater spring) [Ref. 16] are shown at 44°05'08"N, 09°49'31"E and 44°06'11.7"N, 09°49'05"E.

The oldest feature observed in the gulf is the ancient drainage channel that originated subaerially sometime during the Pleistocene epoch. At some point during the rise of sea level in the Holocene (glacial melting) the conditions were such that a cross-gulf barrier-bar was formed by longshore drift of coarse sedimentary material. This material included rounded gravel that resembles present-day beach deposits found near the mouth of the Magra River, 10 km to the southeast. The upper surface of the barrier-bar was once at or near sea level and was covered by vegetation.

The morphology of the barrier-bar and the generally accepted curve of eustatic changes in sea level [Ref. 21] indicate that this was probably about 8000 years ago. Coral grew on the flanks of the bar, a lagoon formed to the landward of it, and "layers" protected from the action of the sea formed in quiet waters of the lagoon. With the further rise in sea level, the dynamic conditions that created the barrier-bar were removed, and the bar and fringing reef coral on its flanks were buried by a cover of fine sedimentary material.

ACKNOWLEDGEMENTS

Many people assisted the authors during this research and their contribution is gratefully acknowledge. Messrs. Kermabon, Blavier, Matteucci, Hastrup, Lallement, Schunk, and Mastrosanti of SACLANTCEN provided assistance at sea. Messrs. Kermabon, Blavier, and Matteucci performed the bulk of the sediment coring and laboratory sedimentalogic data analysis. The authors appreciate the loan of the prototype "Mud Penetrator" from the Institut Océanographique de Monaco, the Clamshell Sediment dredge from the CNEN - EURATOM, Sea-Contamination Research Laboratory at Fiascherino (La Spezia), and the ASW Bomb from the Italian Navy.

REFERENCES

1. L.R. Breslau and H.E. Edgerton, The Sub-Bottom Structure of the Gulf of La Spezia. (A preliminary report) Extrait des Rapports et Procès-Verbaux des Réunions de la C.I.E.S.M.M., Vol. XVIII, Fasc 3, 1965.

2. D. Zaccagna, Descrizione Geologica delle Alpi Apuani. Provveditorato Generale Dello Stato, Roma, Italia, 1932.

3. G. Capellini, Carta Geologica dei Dintorni del Golfo della Spezia e Val di Magra Inferiore. St Cartographico G. Giardi, Firenze, Italia, 1863.

4. Da Portofino Al Gombo. Istituto Idrografico Tirreno, Italia, 1955.

5. Plan du Golfe de La Spezia-Côtes d'Italie (Duché de Gênes). Dépot-Général de la Marine de la Republique Francaise, Paris, France, 1846.

6. Rada di La Spezia. Istituto Idrografico, Tirreno, Italia, 1962.

7. H.E. Edgerton, Instruction Manual for the "Mud Penetrator". EG&G Inc., Boston, Mass.

8. O. Leenhardt, Le Mud Penetrator. Bull. Inst. Ocean., Monaco, 1964.

9. J.A. Yules and H.E. Edgerton, Bottom Sonar Search Techniques. Undersea Tech., 1964.

10. L.R. Breslau, Classification of Sea-Floor Sediments with a Shipborne Acoustical System. La Revue Pétrolière, Paris, France, 1965.

11. L.R. Breslau, The Normally-Incident Reflectivity of the Sea-Floor at 12kc and its Correlation with Physical and Geological Properties of Naturally-Occurring Sediments. Ref.No.67-16, Woods Hole Oceanographic Institution, Woods Hole, Mass., 1967.

12. A. Kermabon, P. Blavier and U. Cortis, The SACLANTCEN "Sphincter" Corer Assembly. SACLANT ASW Research Centre Technical Report No. 34, March 1965. (NATO UNCLASSIFIED)

13. E.C. Forzani, Relazioni Intorno di Principali Lavori Arsenale Militare Marittimo di Spezia. Tipografi del Senato, Roma, Italia, 1881.

14. H.E. Edgerton, Sub-Bottom Penetrations in Boston Harbour. J. Geophysical Res., 1963.

15. W. Rasmussen and L. Breslau, Hydrography and Water Supply Lakes Ao Ho and Bau Ro, Can Ranh Peninsula, RVN, OICC, Naval Facilities Engineering Command, Saigon, Vietnam, 1968

16. D. Zaccagna, La Geologia del Golfo della Spezia. Accademia Lunigianese di Scienze, La Spezia, Italy 1935.

17. R.R. Shrock, Sequence in Layered Rocks. McGraw-Hill Book Co., New York, 1948.

18. A. Kermabon and U. Cortis, A Recoilless Piston for the SACLANTCEN "Sphincter" Corer. SACLANT ASW Research Centre Technical Report No. 113, April 1968. (NATO UNCLASSIFIED)

19. A. Johansen, An Acoustic, High-Resolution, Sediment Profiler. SACLANT ASW Research Centre Technical Report No. 72, November 1966. (NATO UNCLASSIFIED).

20. A. Kermabon, C. Gehin and P. Blavier, A Deep-Sea Electrical-Resistivity Probe. SACLANT ASW Research Centre Technical Report No. 115, April 1968. (NATO UNCLASSIFIED)

21. R.W. Fairbridge, Eustatic Changes in Sea Level, Physics and Chemistry of the Earth. Prentice-Hall, New York, 1961.

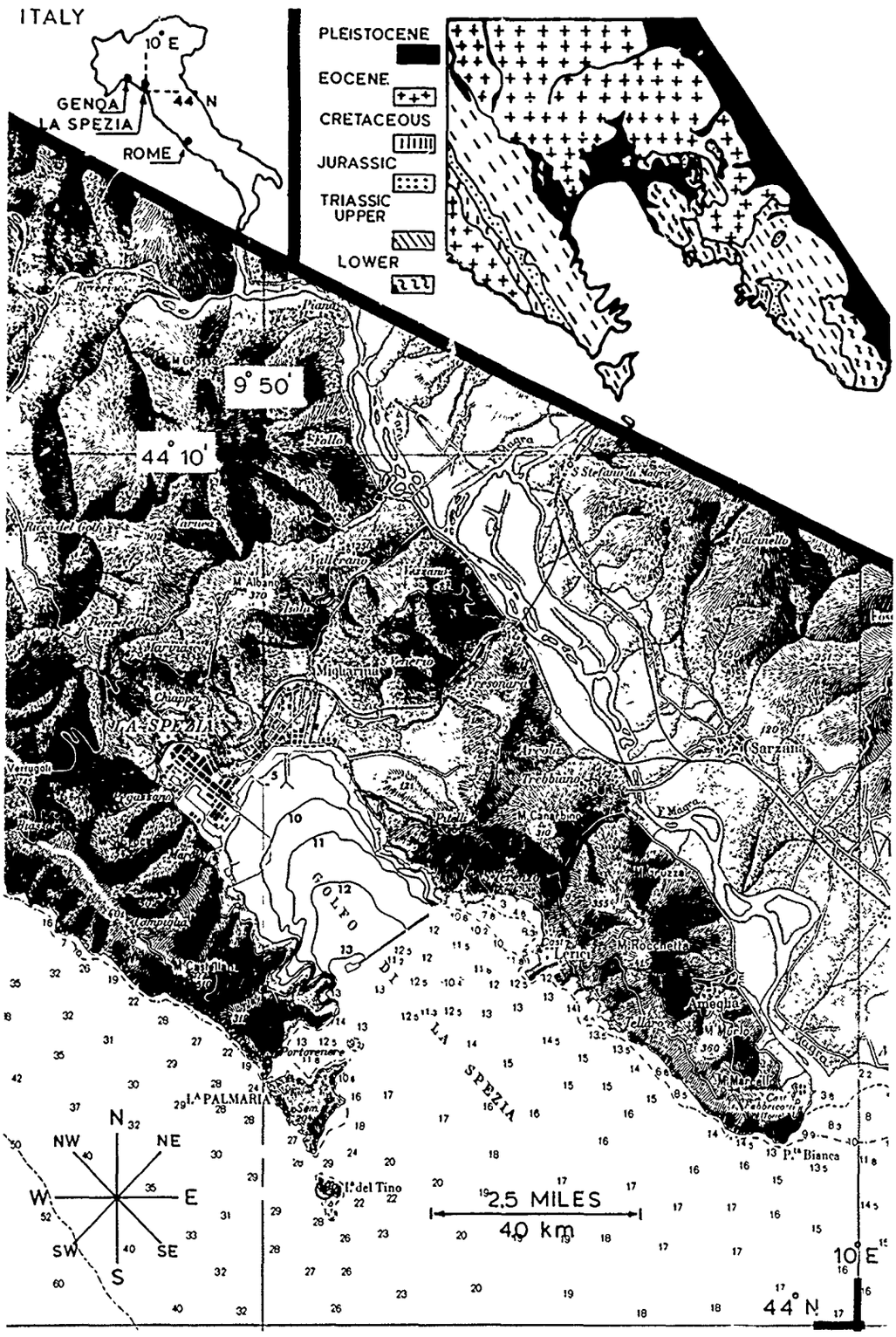

FIG. 1 LOCATION, GEOLOGY, AND RELIEF OF THE ENVIRONS OF THE GULF OF LA SPEZIA

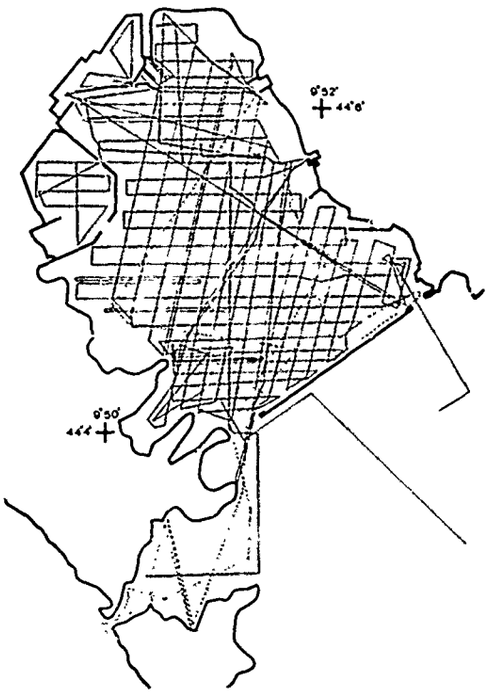

FIG. 2a CRUISE TRACKS OF THE FIRST SURVEY
(rough navigation)

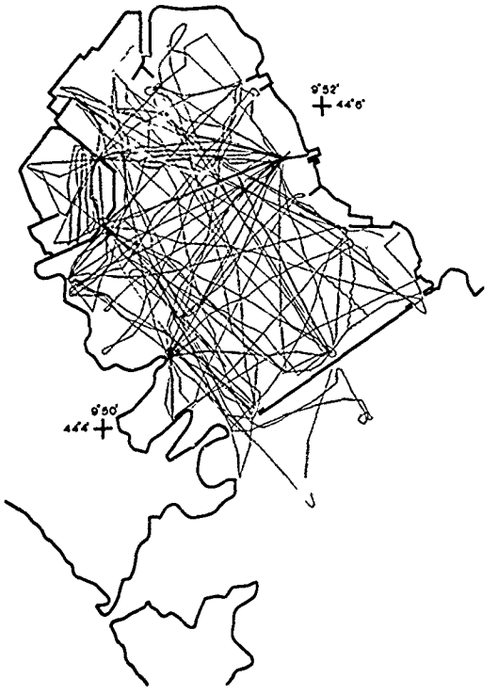

FIG. 2b CRUISE TRACKS OF THE SECOND SURVEY
(fine navigation)

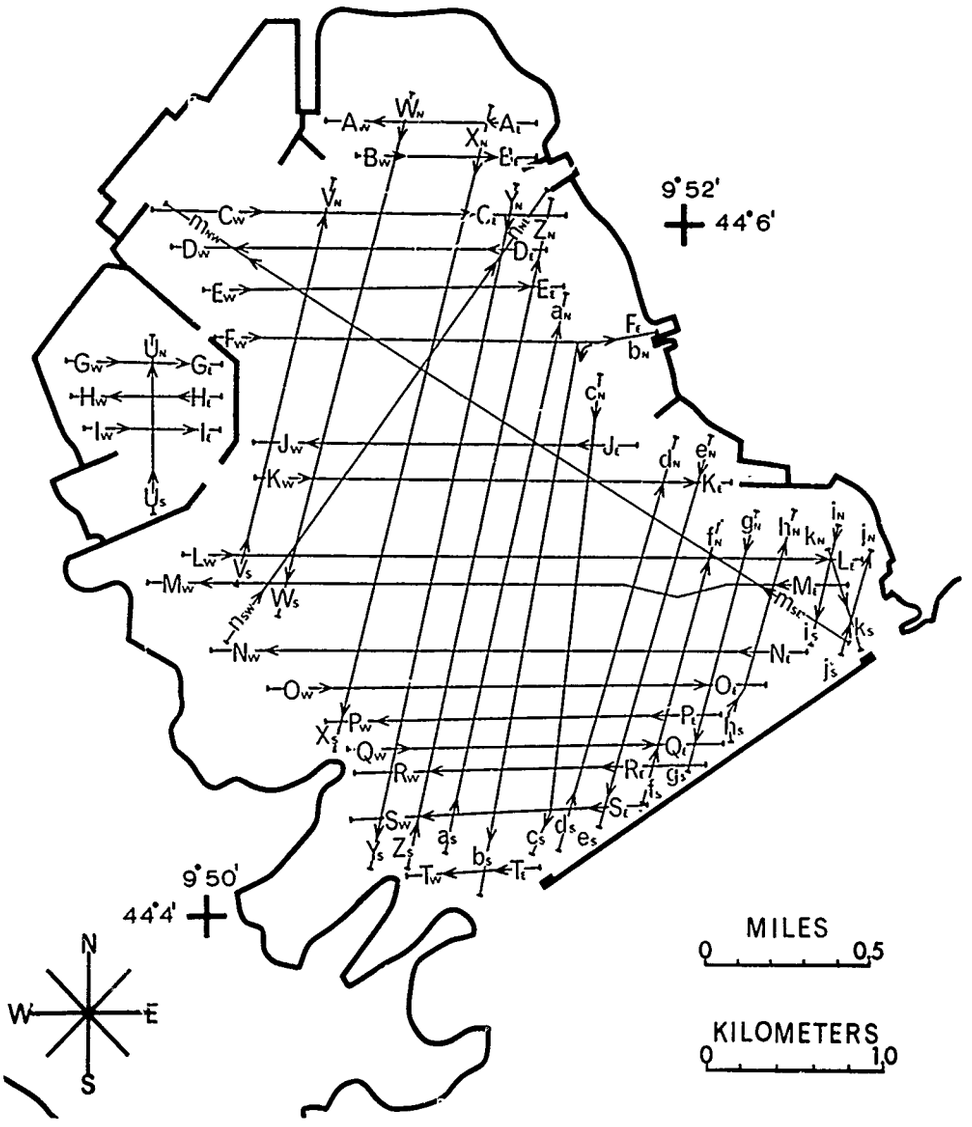

FIG. 3 LOCATION OF SELECTED SEISMIC PROFILES

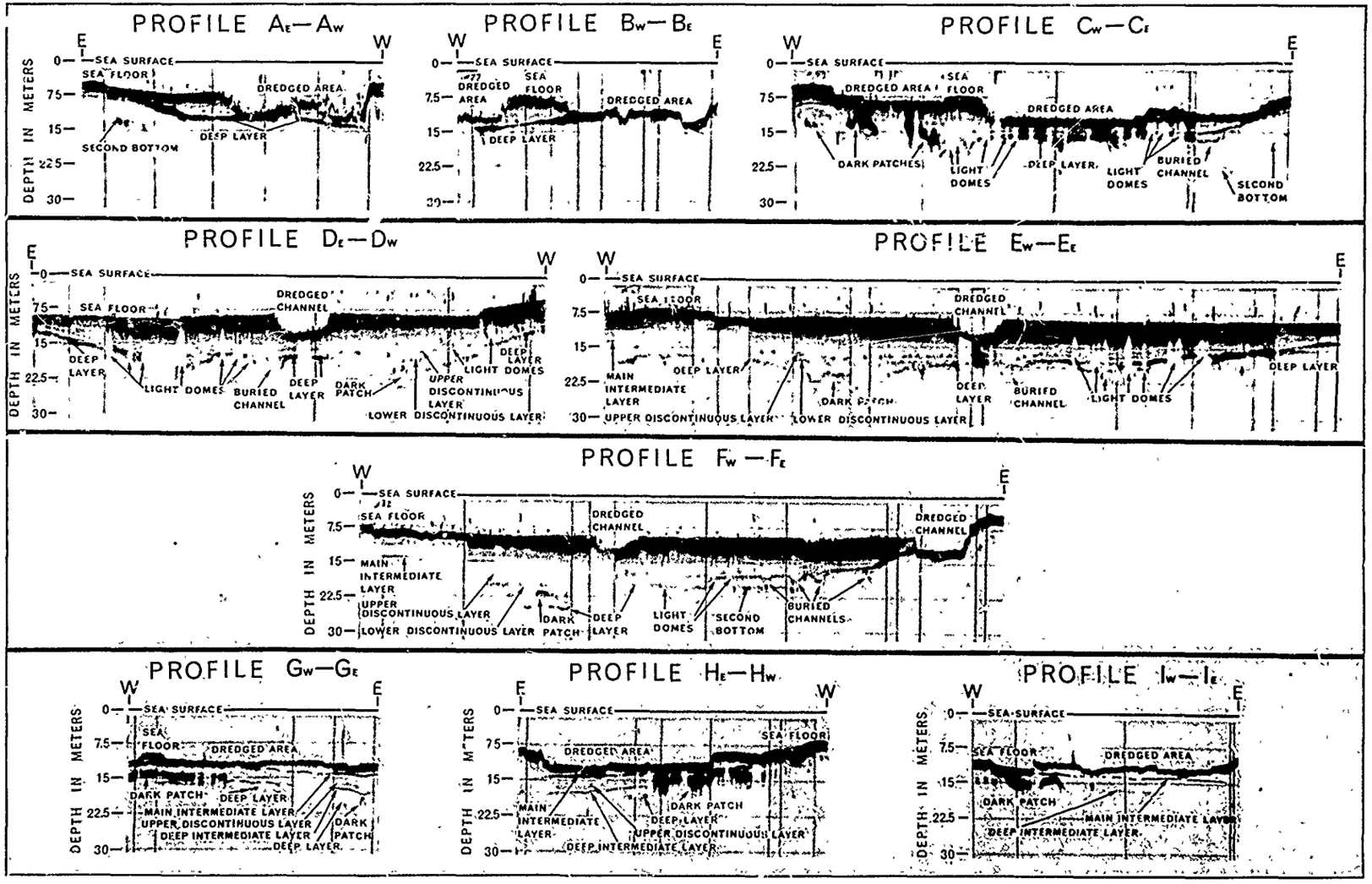

FIG. 4 SELECTED SEISMIC PROFILES (A–I)

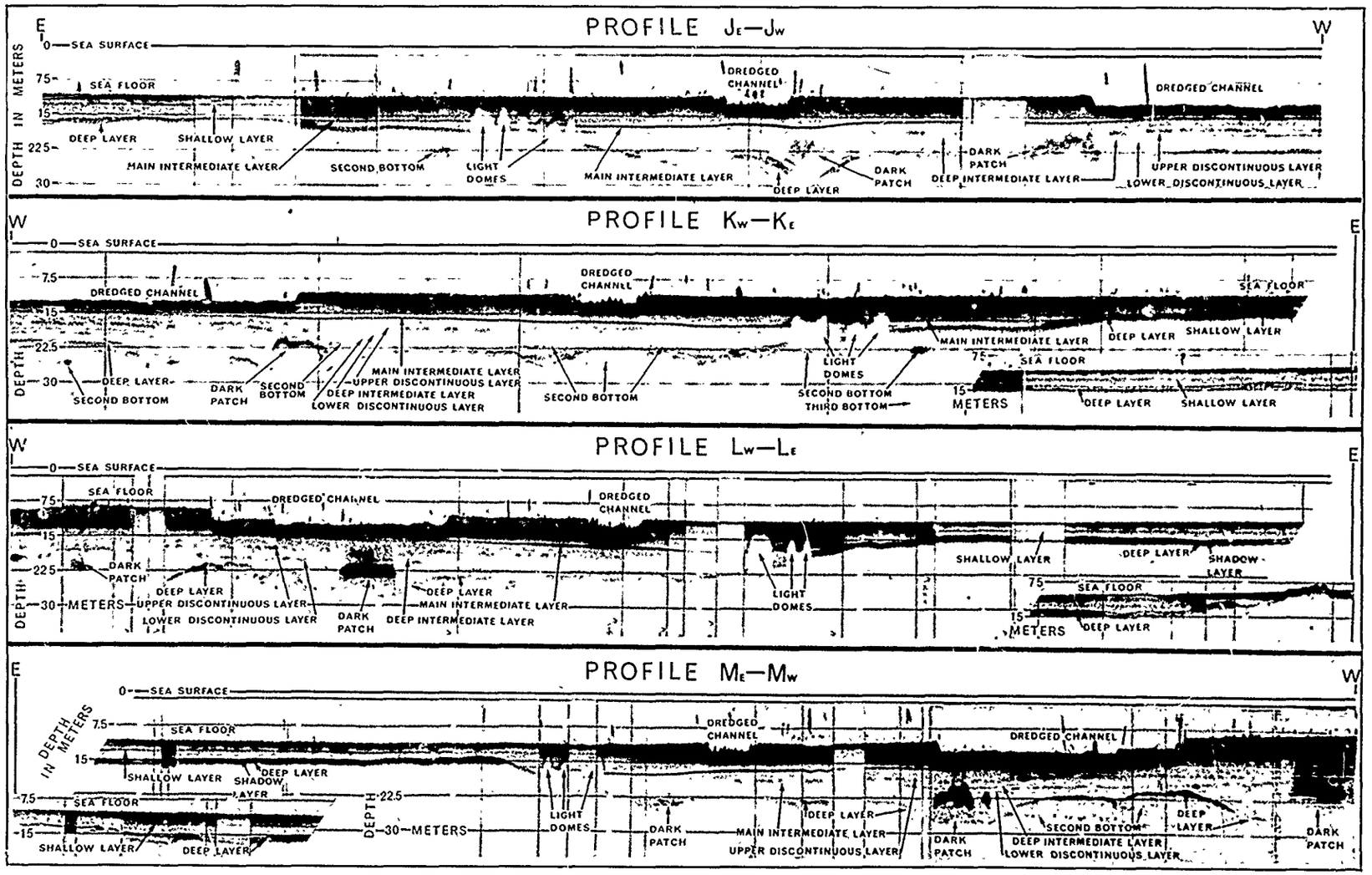

FIG. 5 SELECTED SEISMIC PROFILES (J–M)

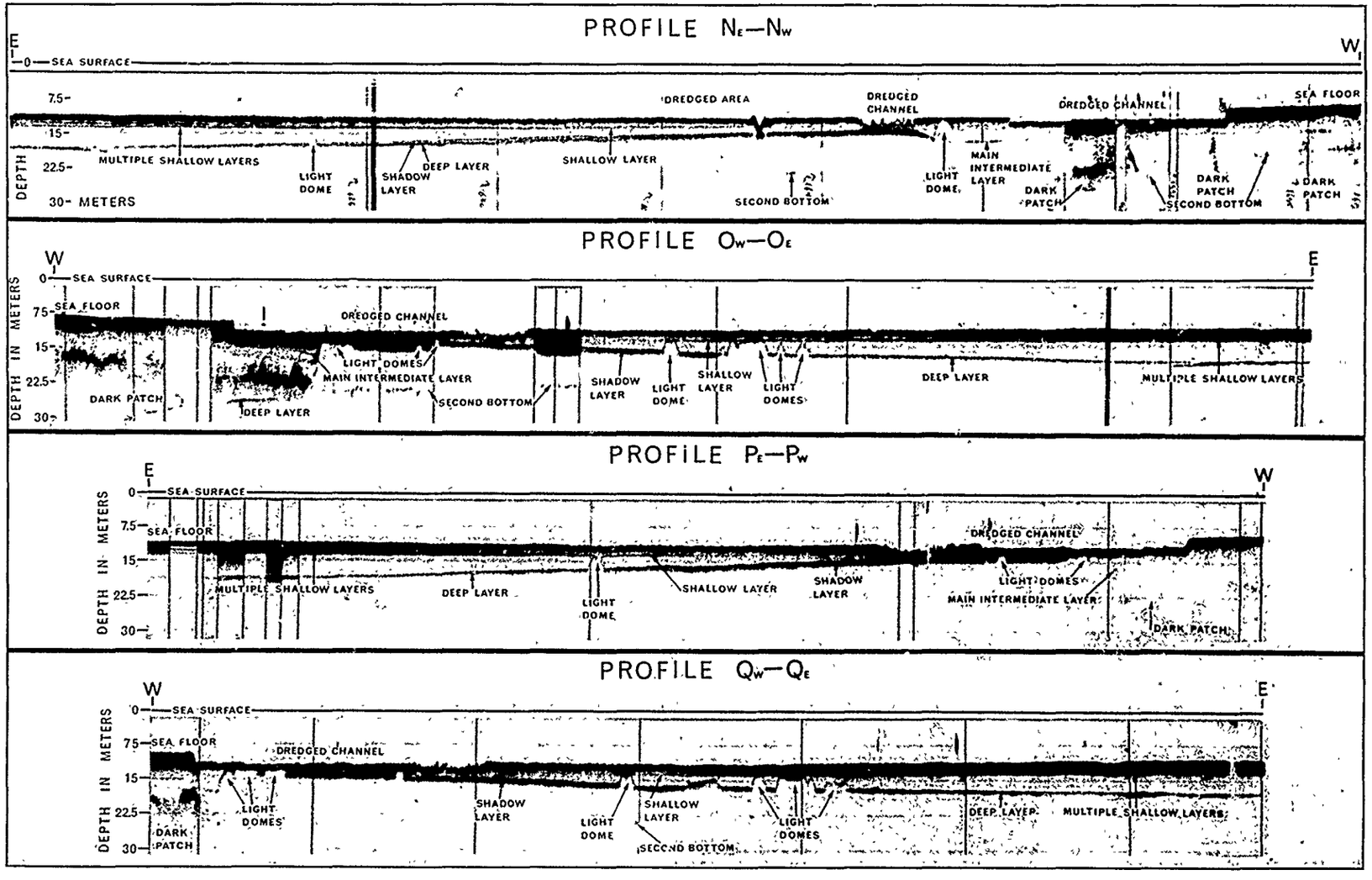

FIG. 6 SELECTED SEISMIC PROFILES (N–Q)

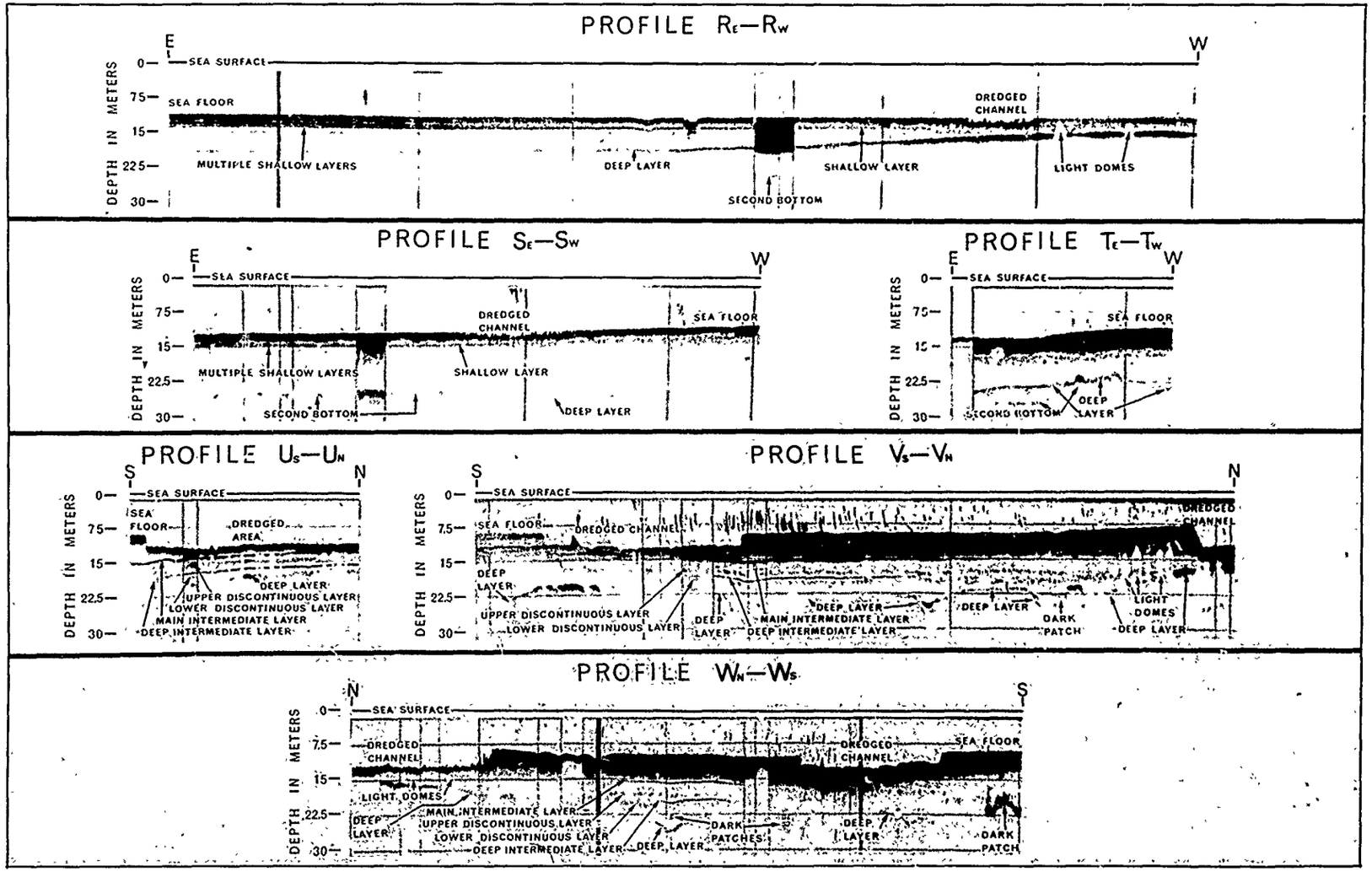

FIG. 7 SELECTED SEISMIC PROFILES (R–W)

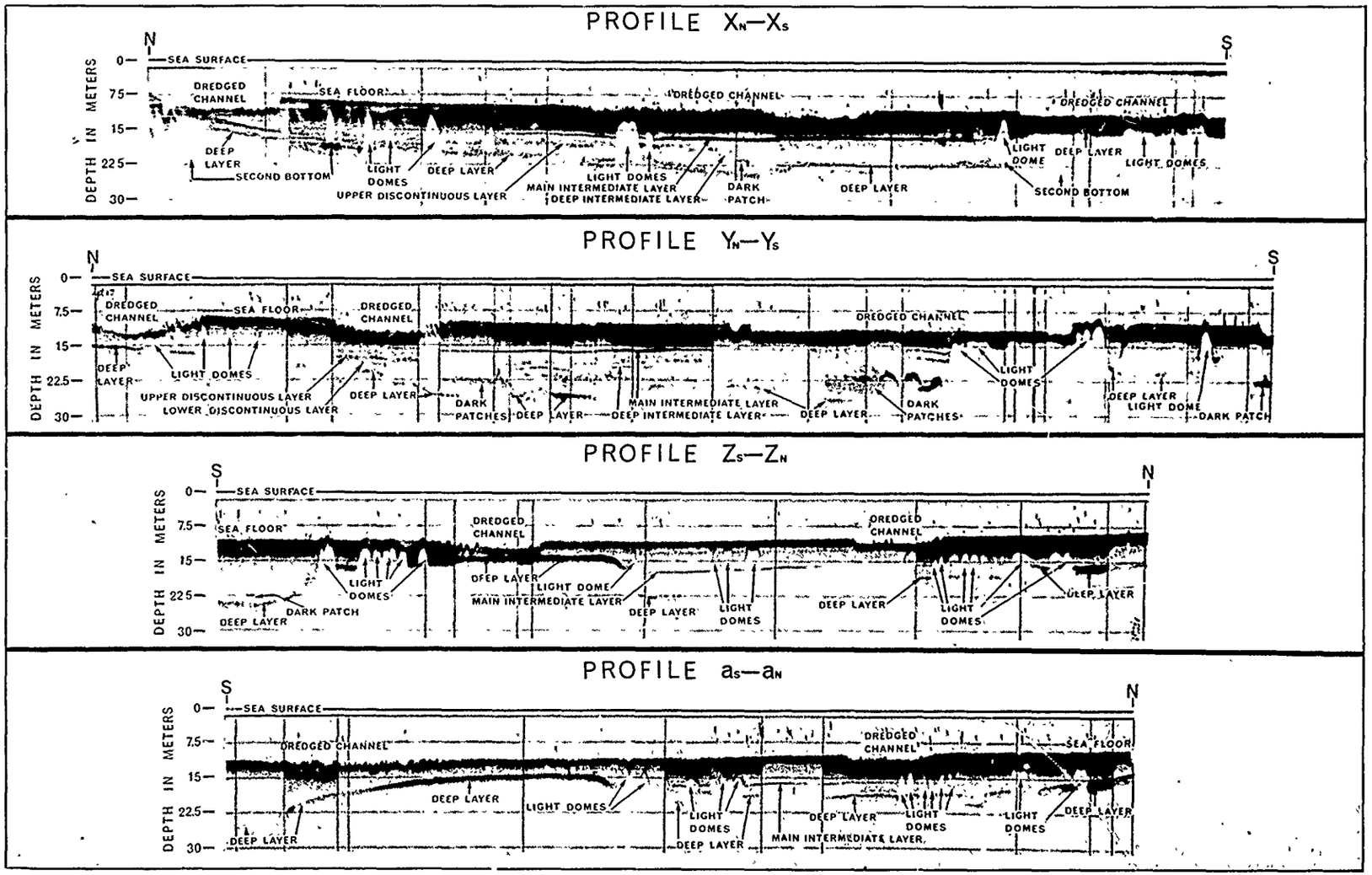

FIG. 8 SELECTED SEISMIC PROFILES (X–a)

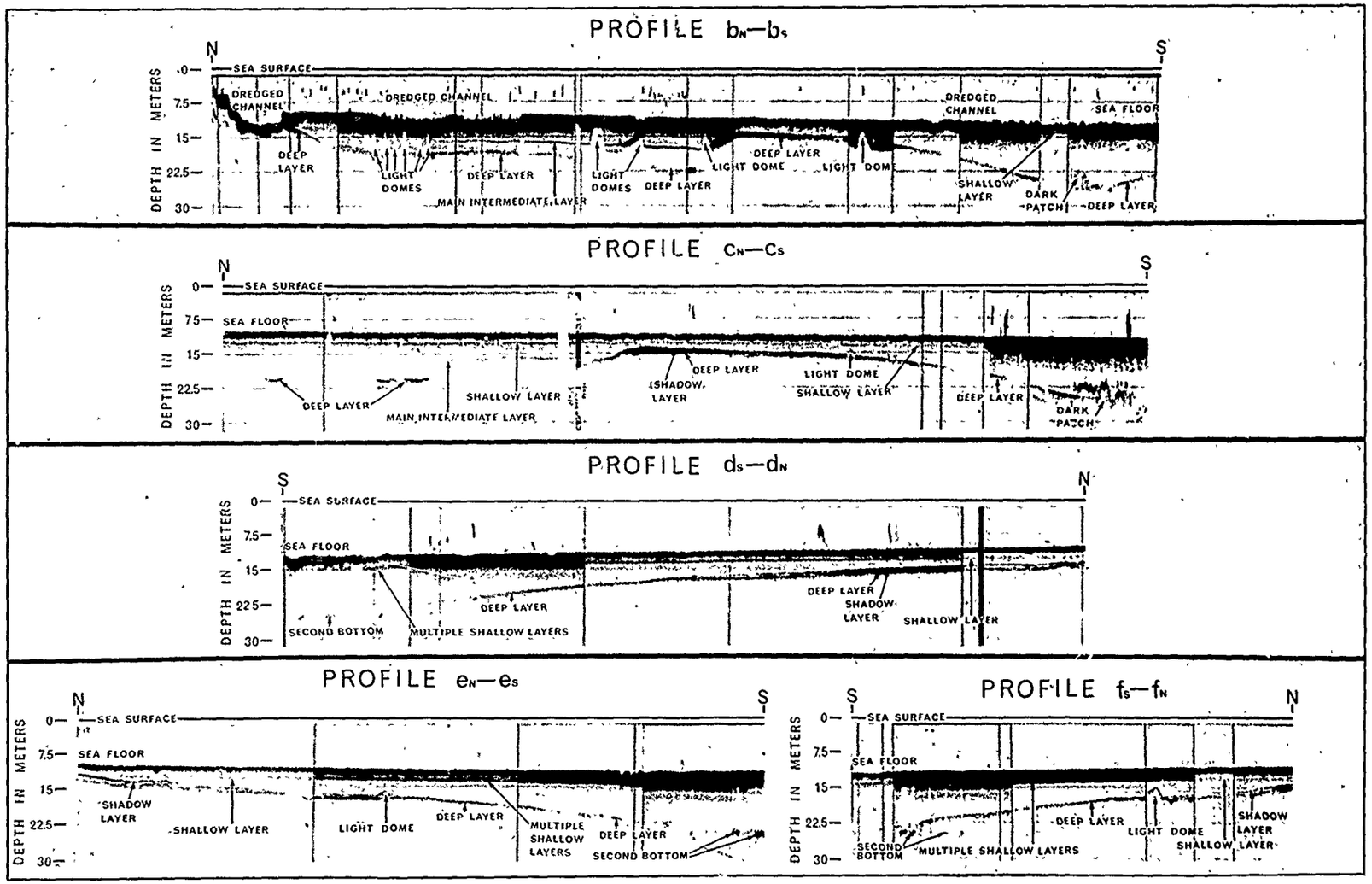

FIG. 9 SELECTED SEISMIC PROFILES (b–f)

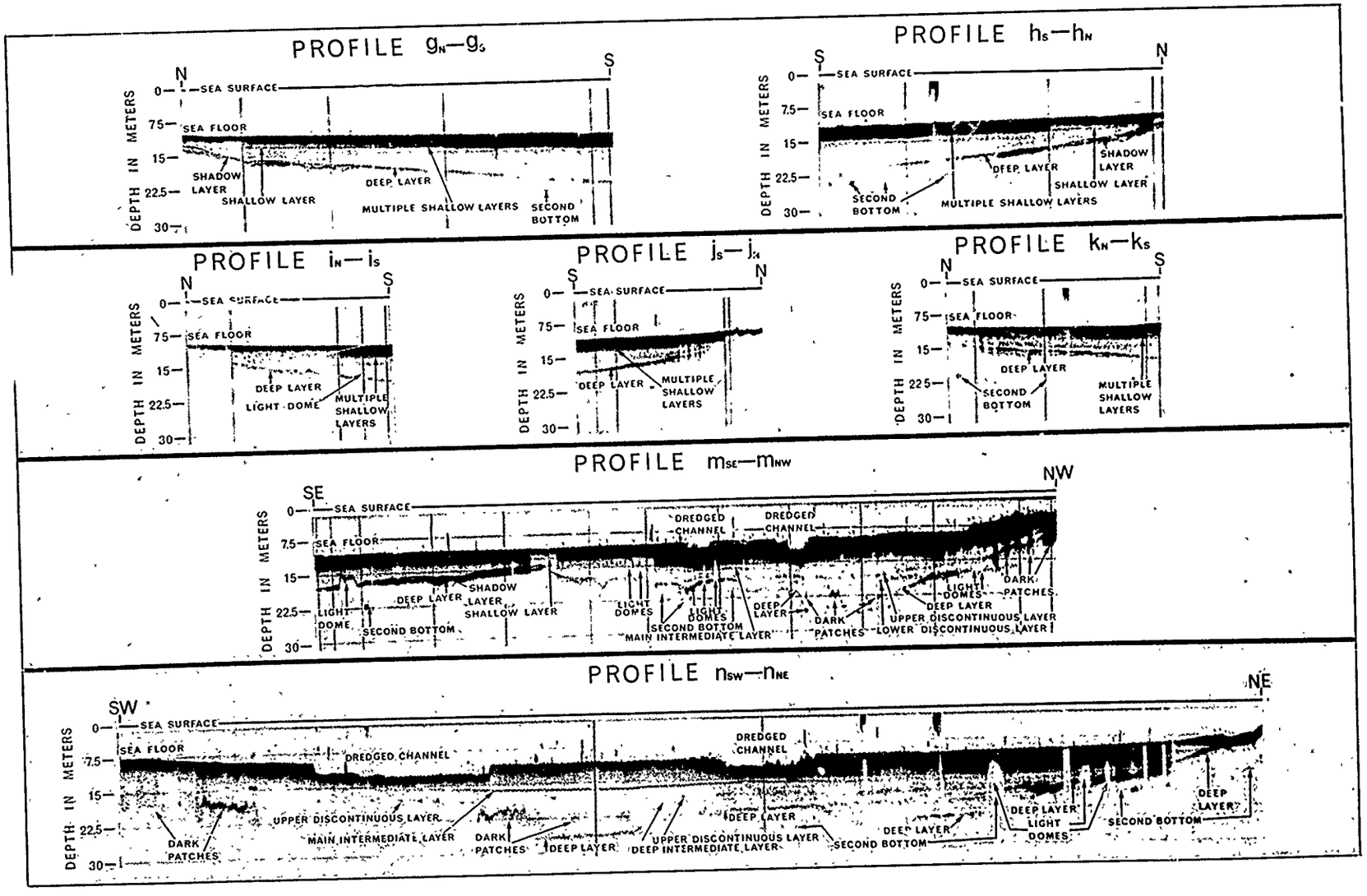

FIG. 10 SELECTED SEISMIC PROFILES (g–n)

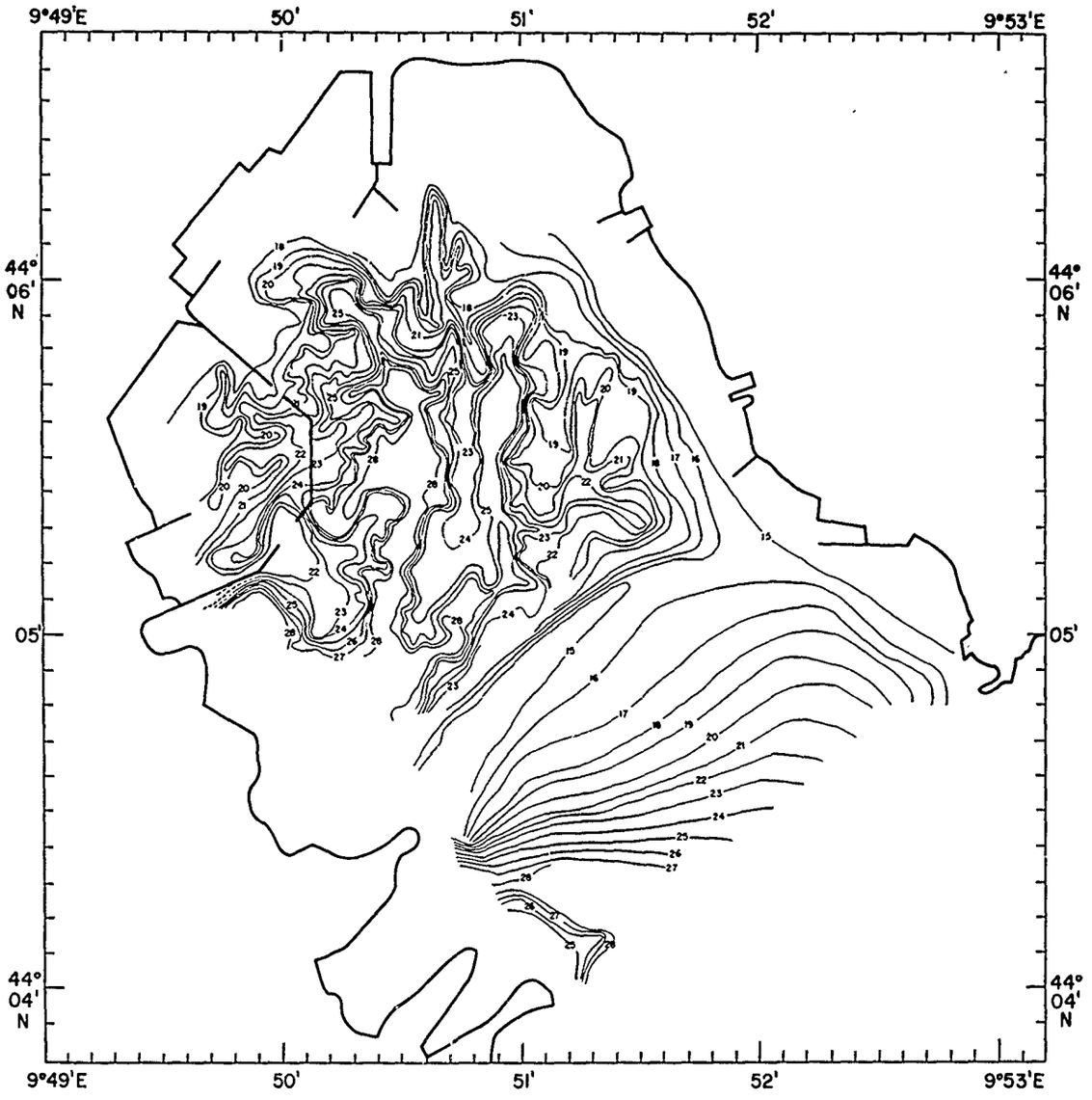

FIG. 11 CONTOURS (in metres) OF DEEP LAYER (terminal layer)

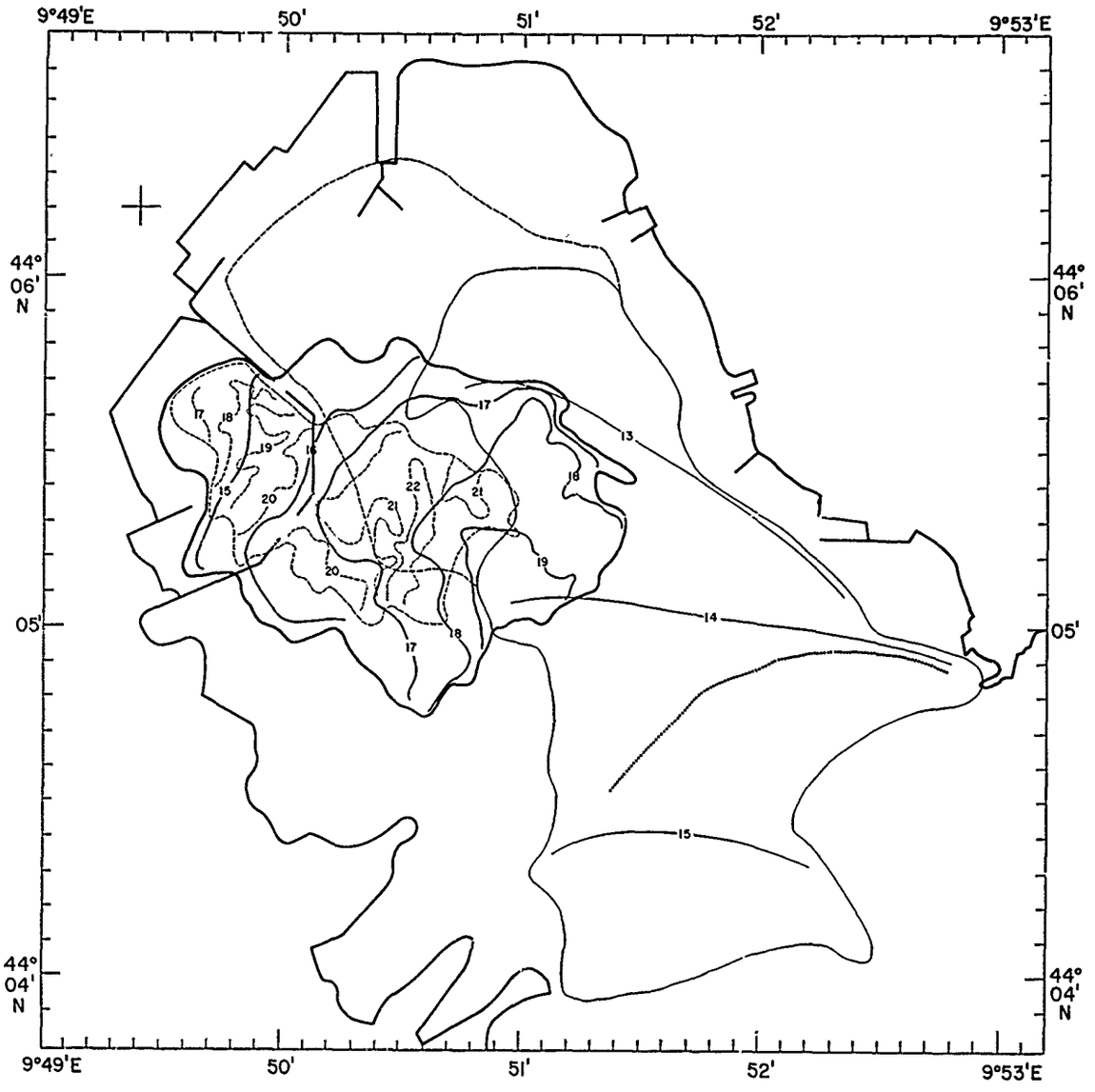

FIG. 12d COMBINED PLOT OF Figures 12a, 12b, and 12c

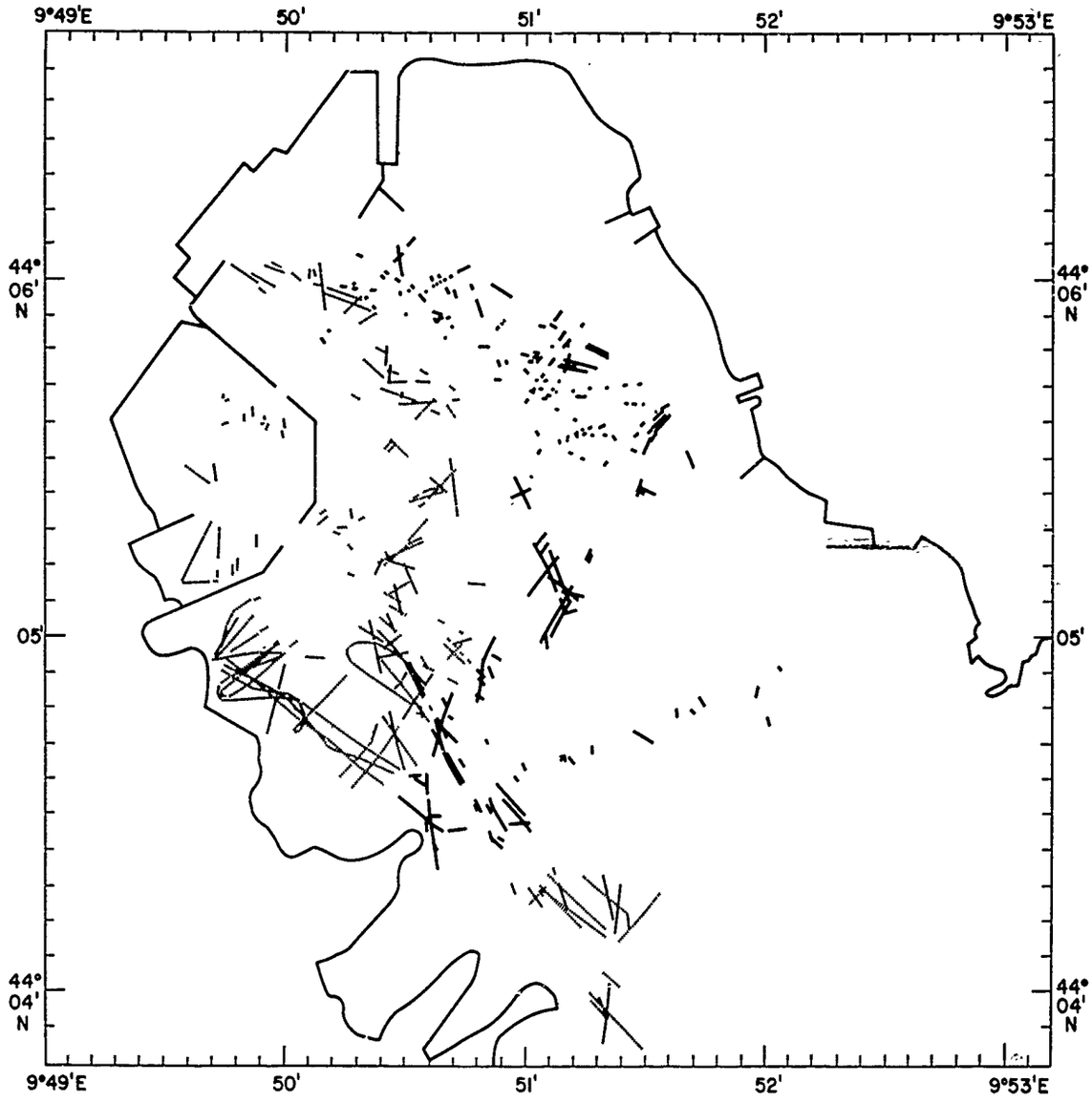

FIG. 13 AREAL DISTRIBUTION OF LIGHT DOMES AND DARK PATCHES

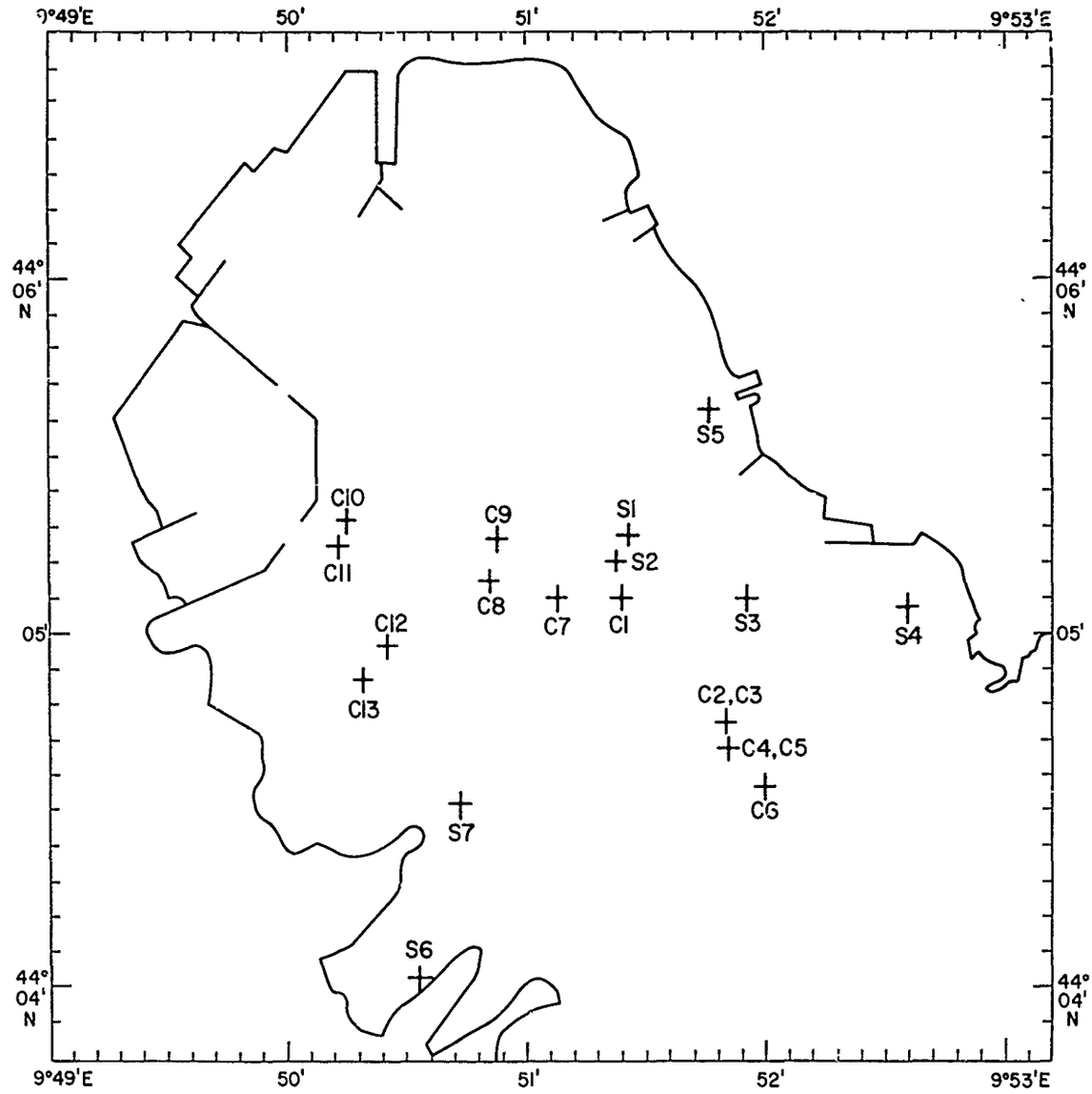

FIG. 14 LOCATIONS OF SEDIMENT CORES AND SURFACE SEDIMENT SAMPLE SITES

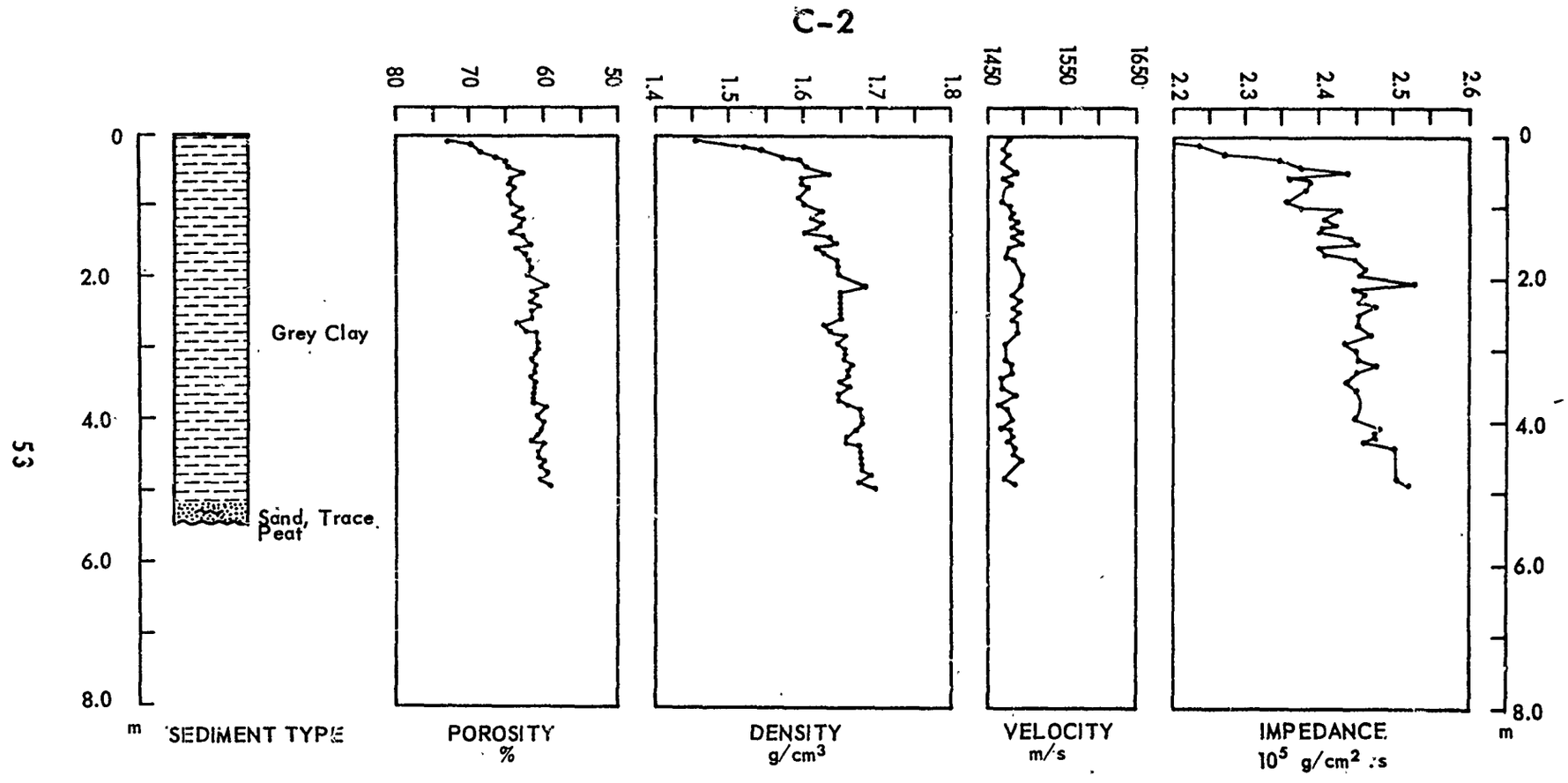

FIG. 15 SEDIMENT CORE C2 ANALYZED FOR SEDIMENT TYPE, POROSITY, DENSITY, SOUND VELOCITY, AND ACOUSTIC IMPEDANCE

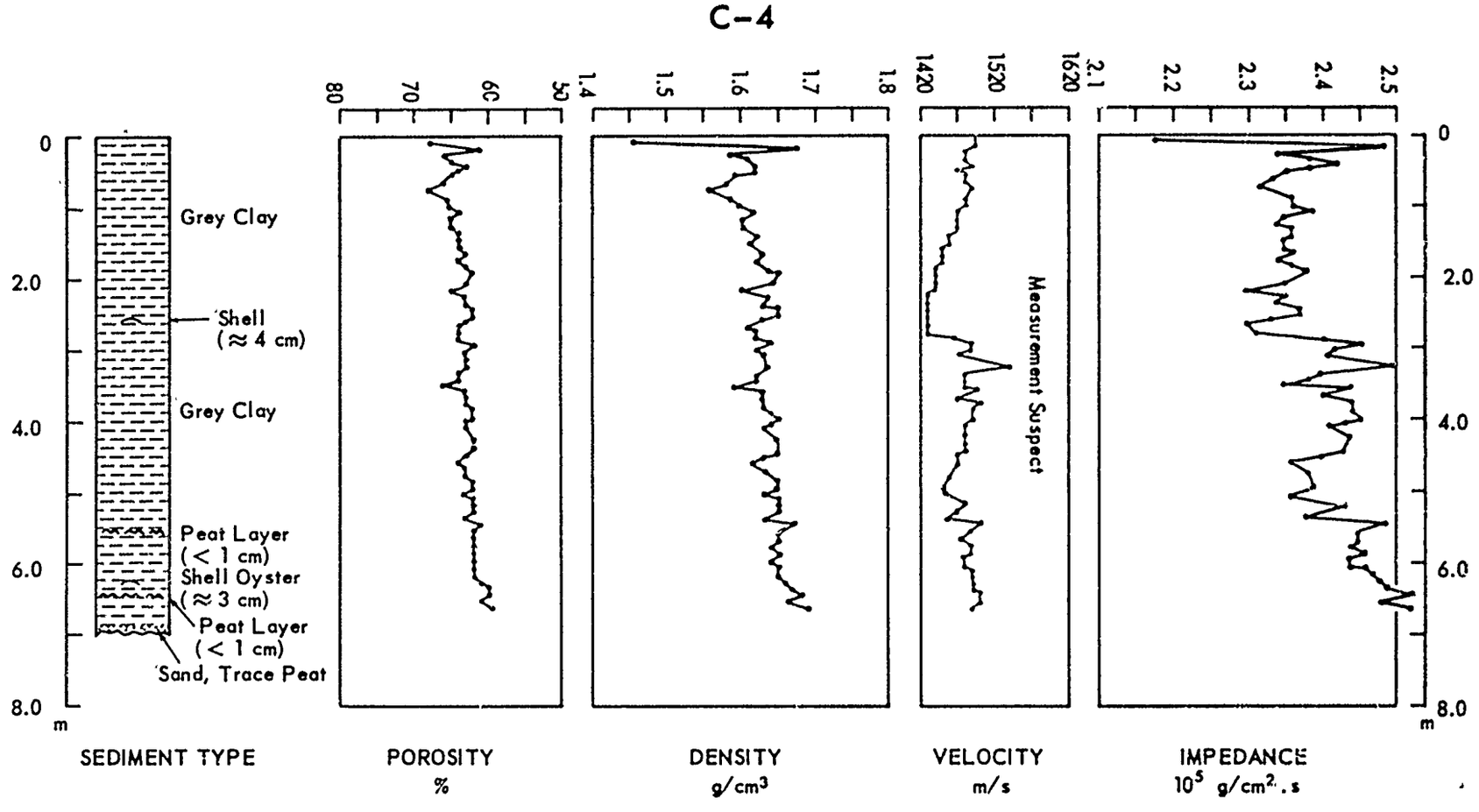

FIG. 16 SEDIMENT CORE C4 ANALYZED FOR SEDIMENT TYPE, POROSITY, DENSITY, SOUND VELOCITY, AND ACOUSTIC IMPEDANCE

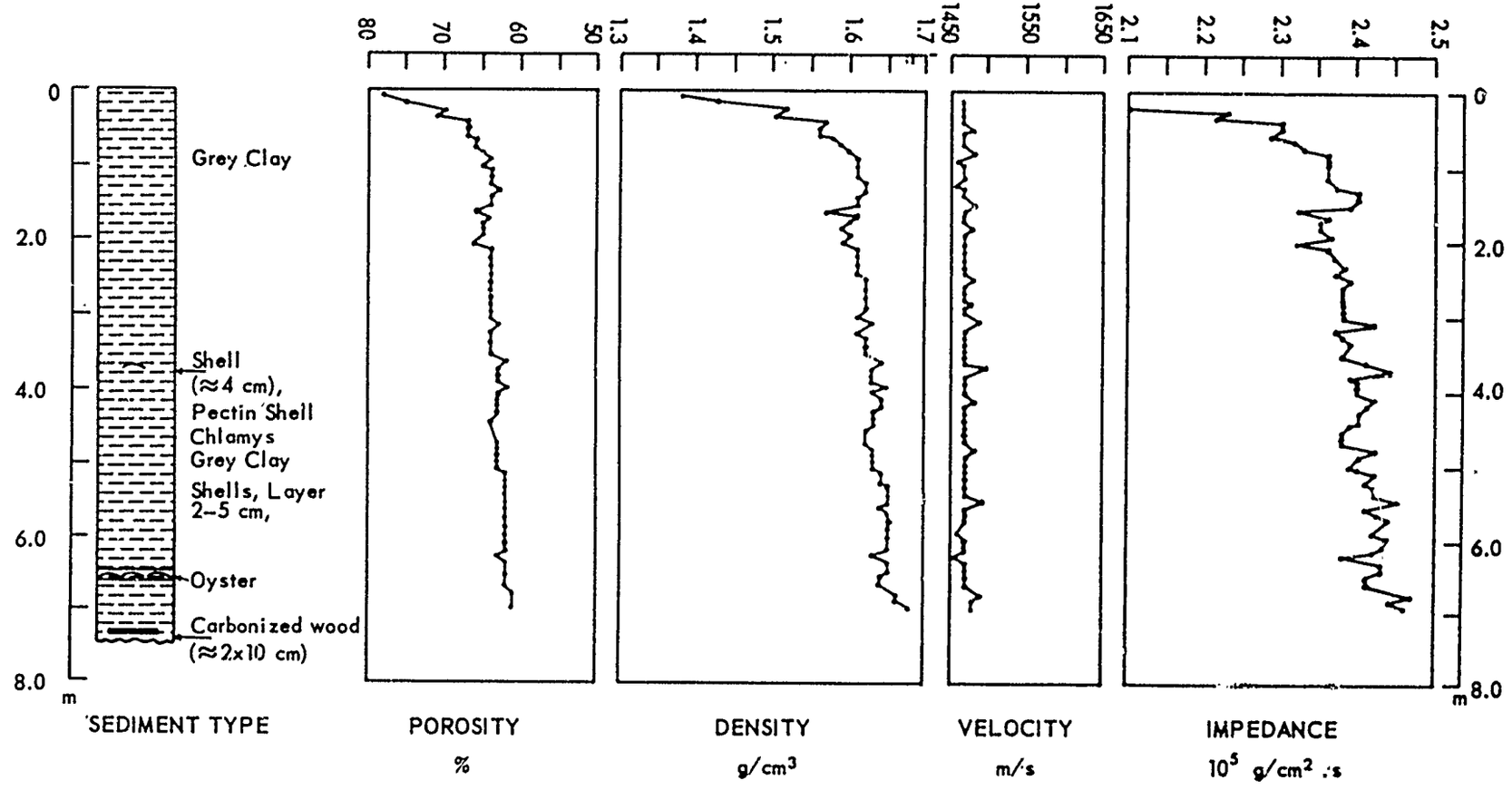

FIG. 17 SEDIMENT CORE C11 ANALYZED FOR SEDIMENT TYPE, POROSITY, DENSITY, SOUND VELOCITY, AND ACOUSTIC IMPEDANCE

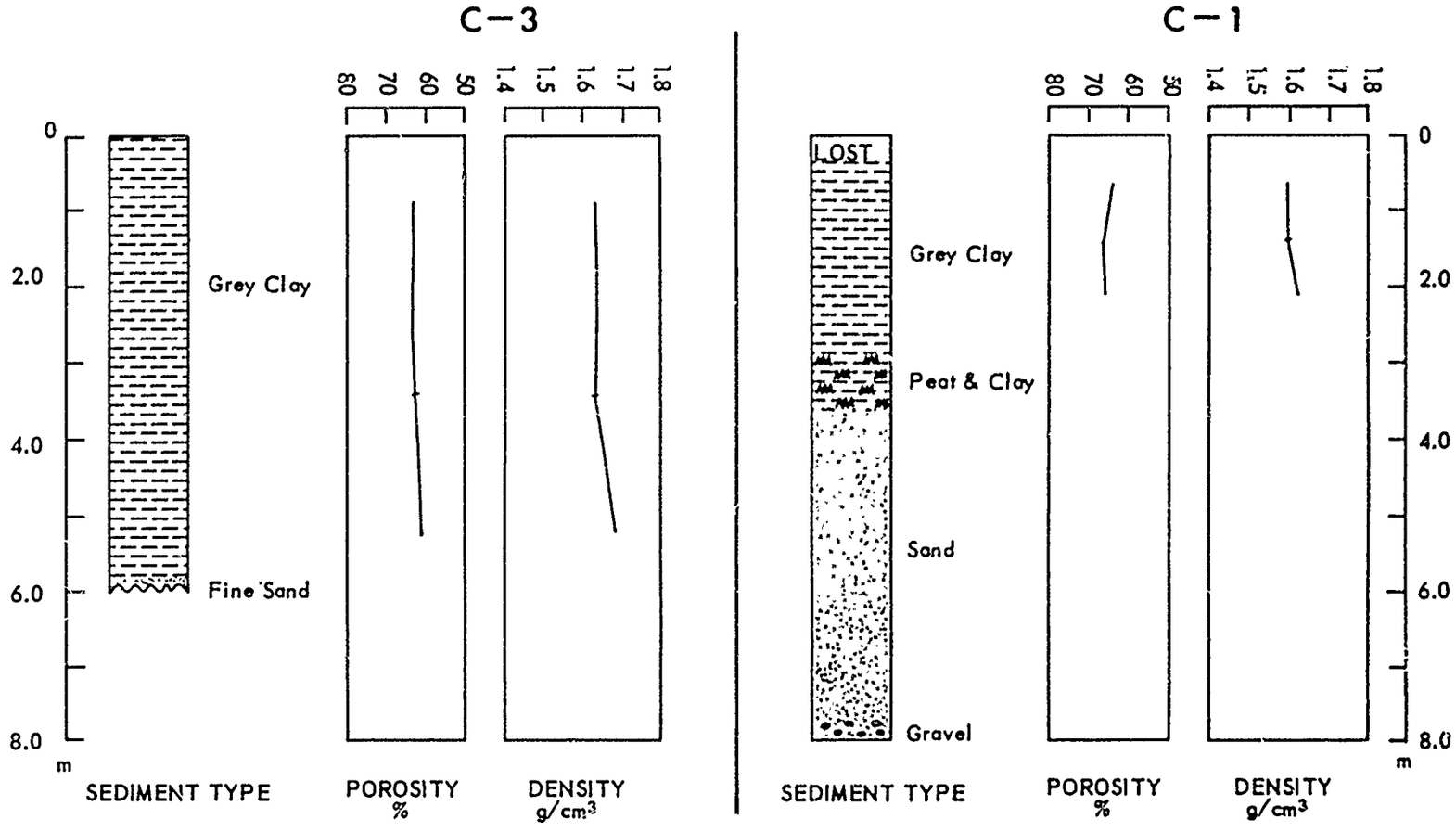

FIG. 18 SEDIMENT CORES C1 AND C3 ANALYZED FOR SEDIMENT TYPE, POROSITY, AND DENSITY

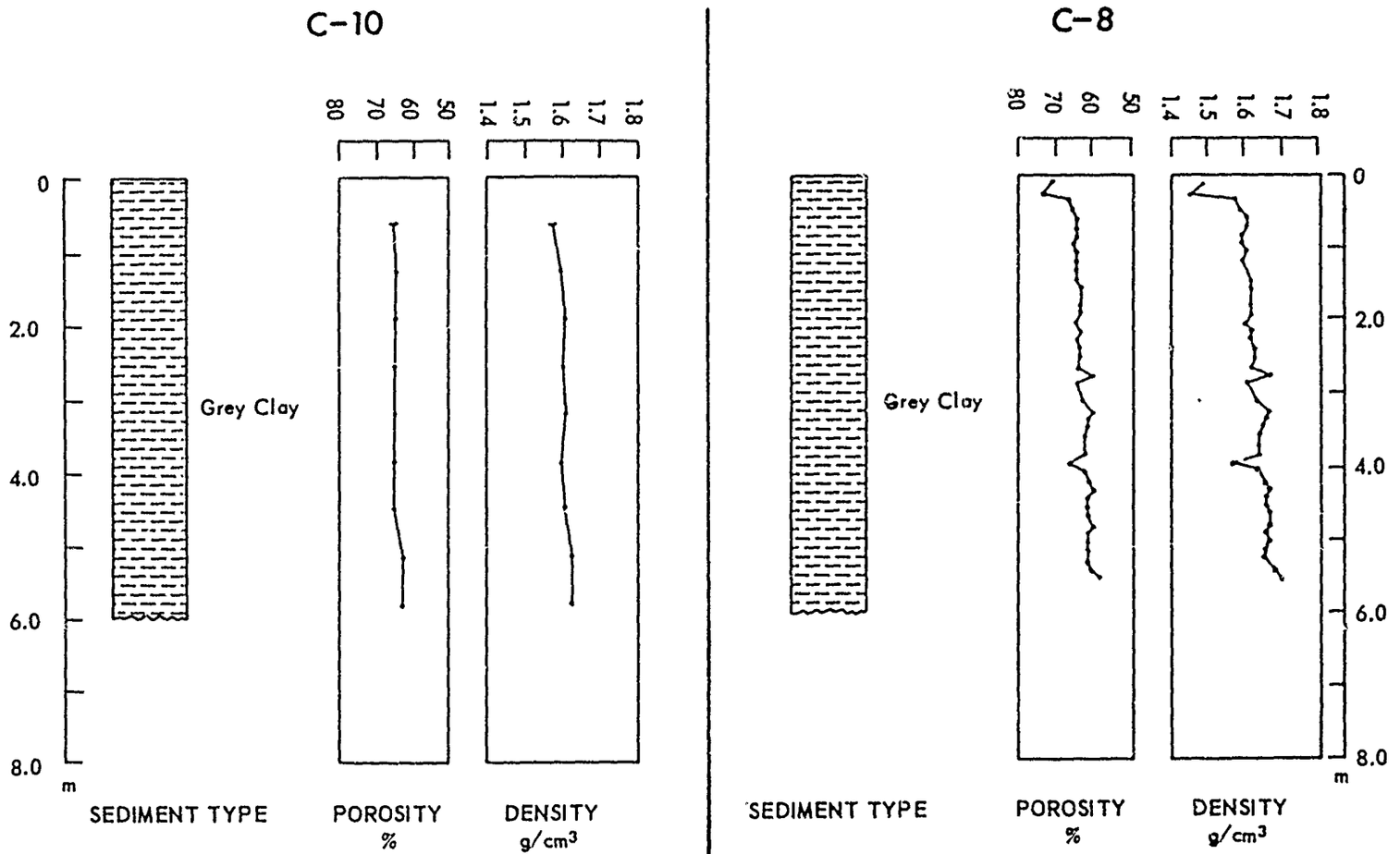

FIG. 19 SEDIMENT CORES C8 AND C10 ANALYZED FOR SEDIMENT TYPE, POROSITY, AND DENSITY

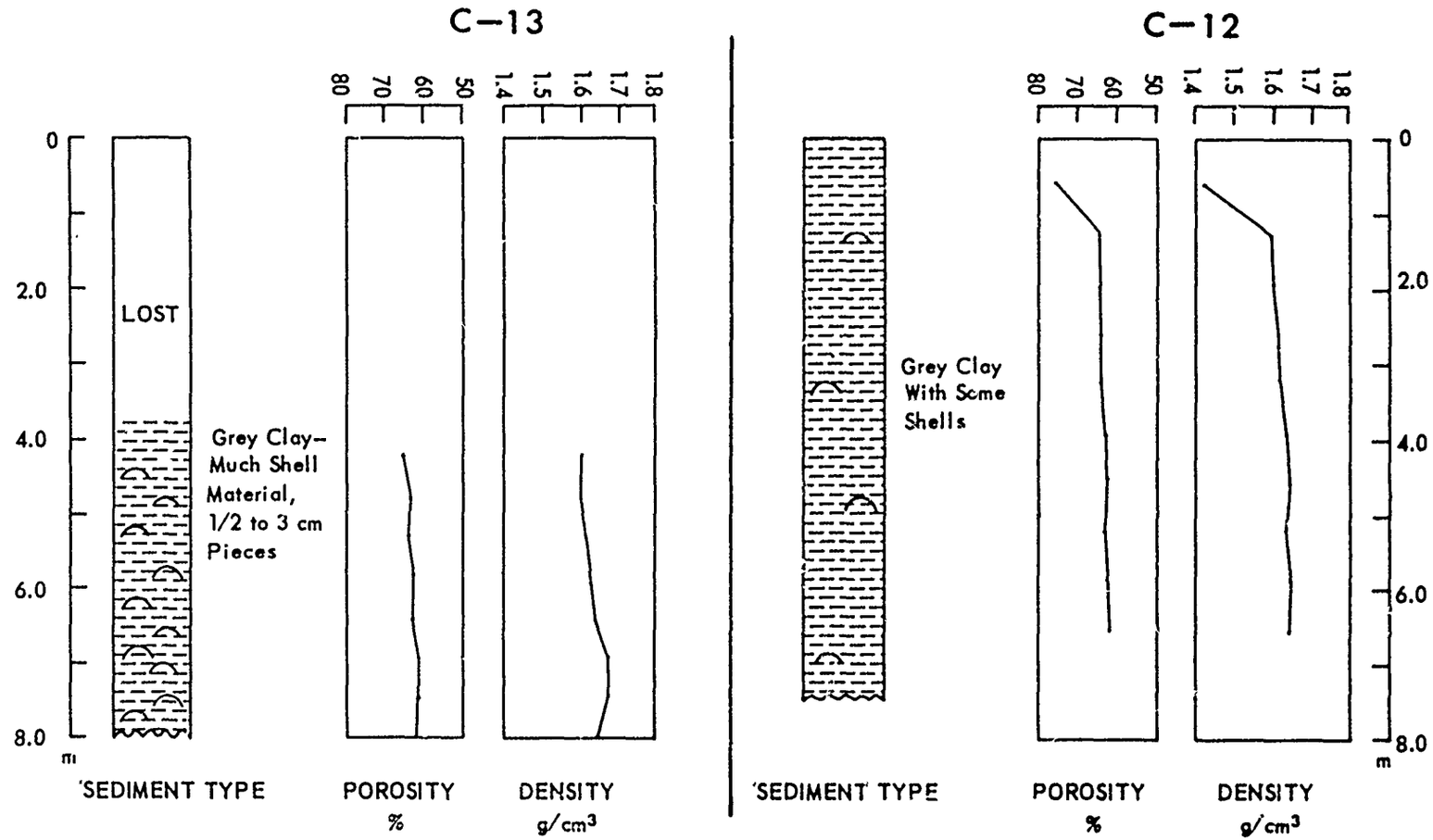

FIG. 20 SEDIMENT CORES C12 AND C13 ANALYZED FOR SEDIMENT TYPE, POROSITY, AND DENSITY

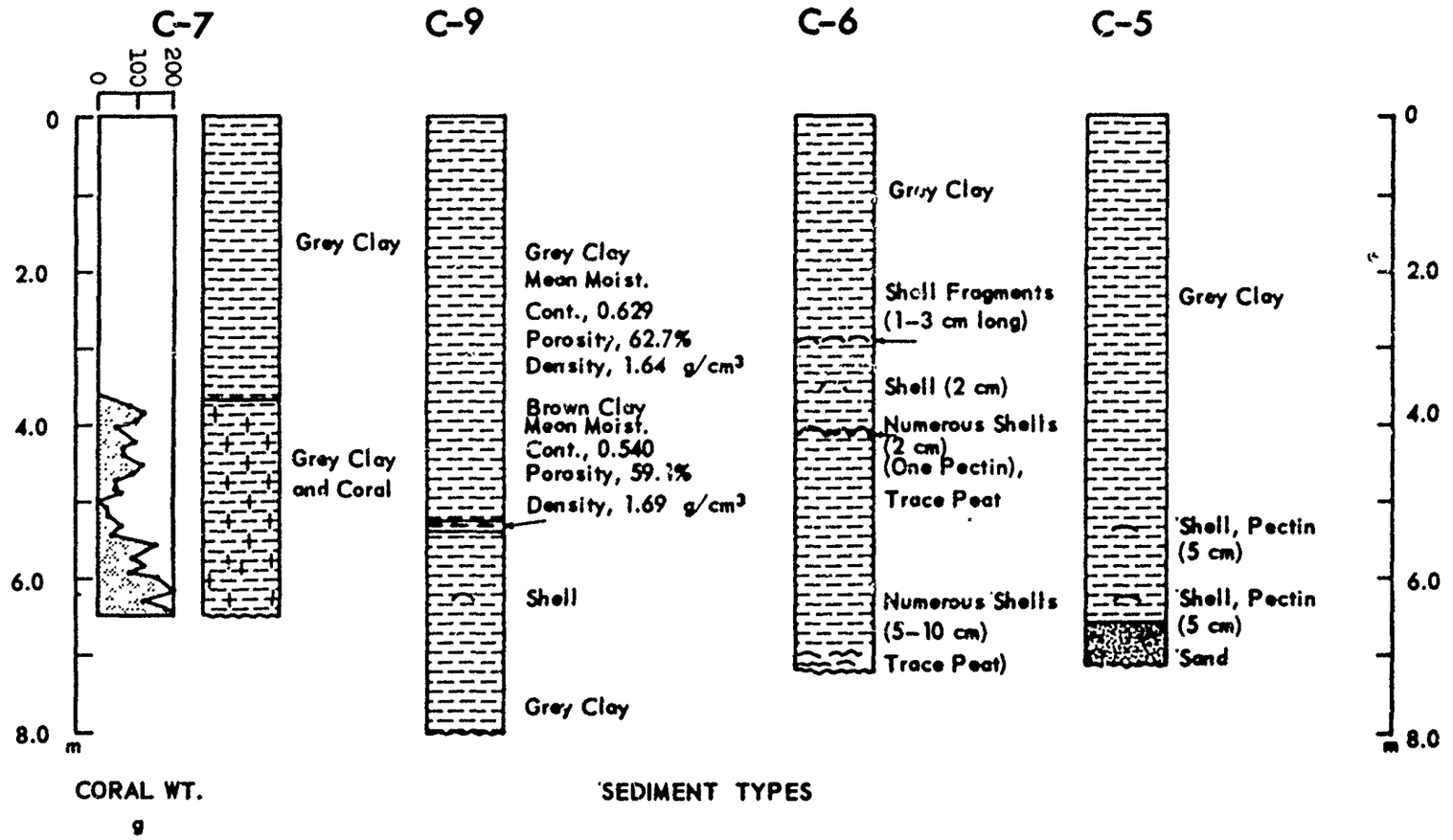

FIG. 21 SEDIMENT CORES C5, C6, C7, AND C9 ANALYZED FOR SEDIMENT TYPE

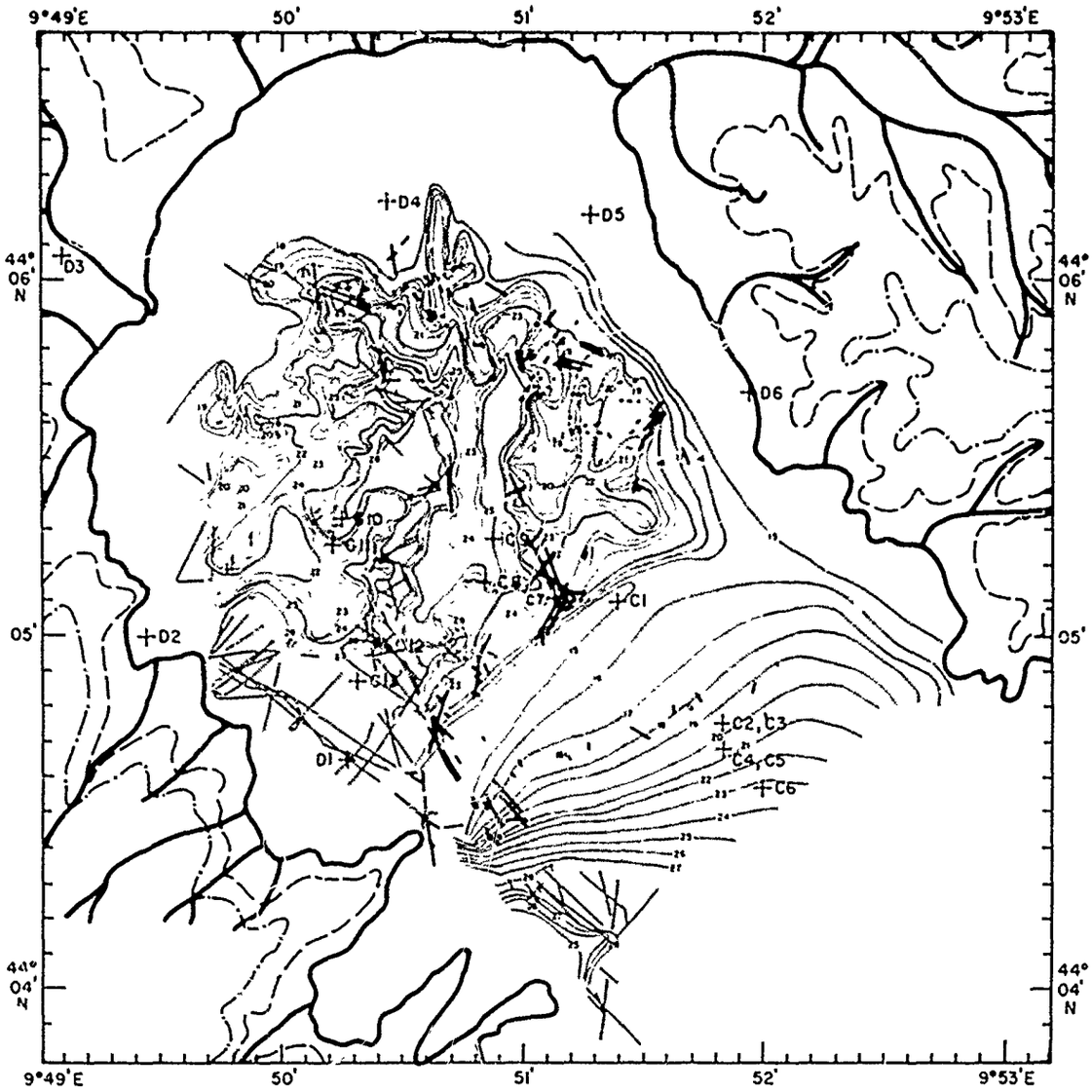

FIG. 22 COMPOSITE DISPLAY OF DEEP LAYER, LIGHT DOMES, DARK PATCHES, AND SEDIMENT SITES (cf Figures 11, 13, and 14)

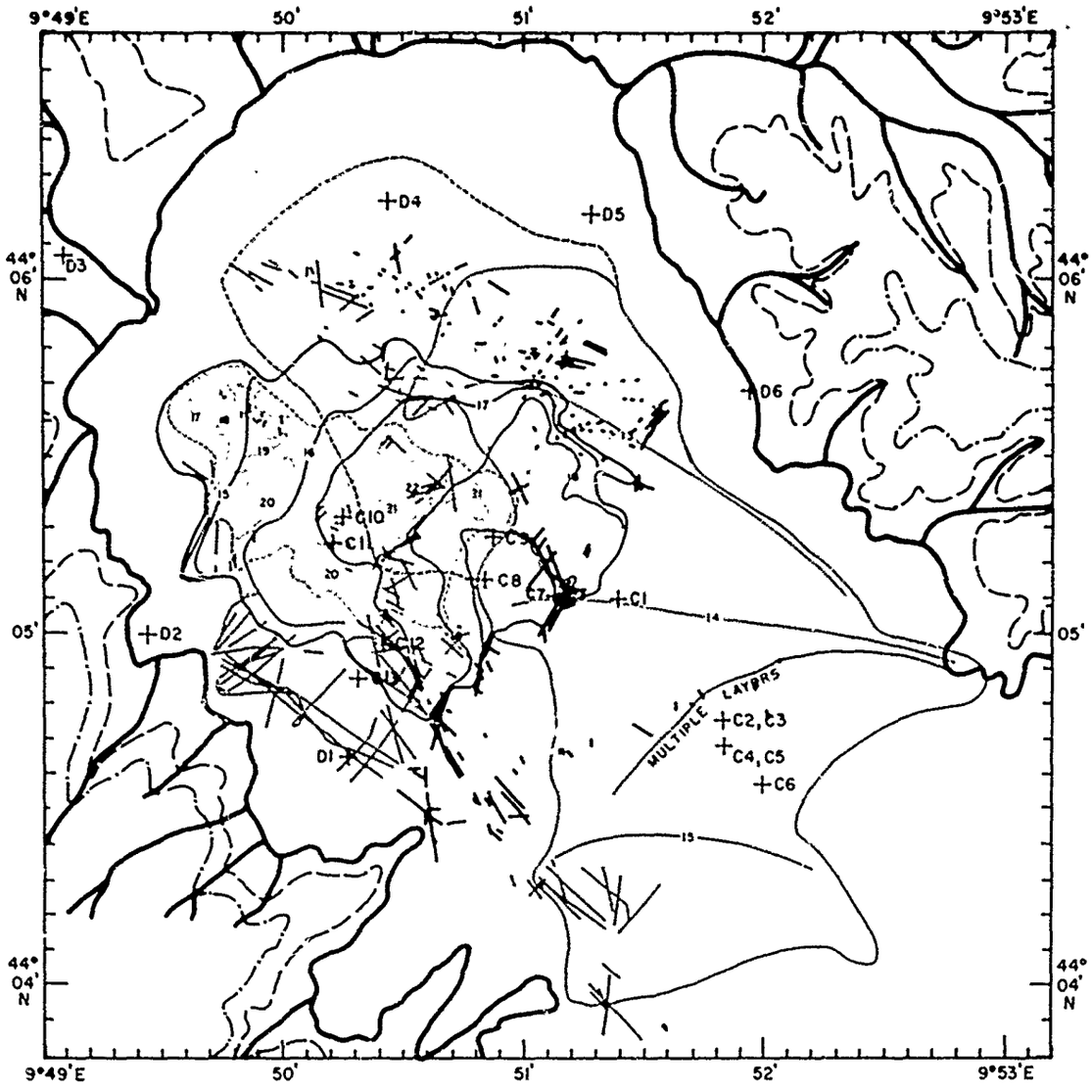

FIG. 23 COMPOSITE DISPLAY OF INTERMEDIATE LAYER, LIGHT DOMES, DARK PATCHES. AND SEDIMENT SITES (cf Figures 12, 13, and 14)

HORIZONTAL (W-E) STANDARD SECTION

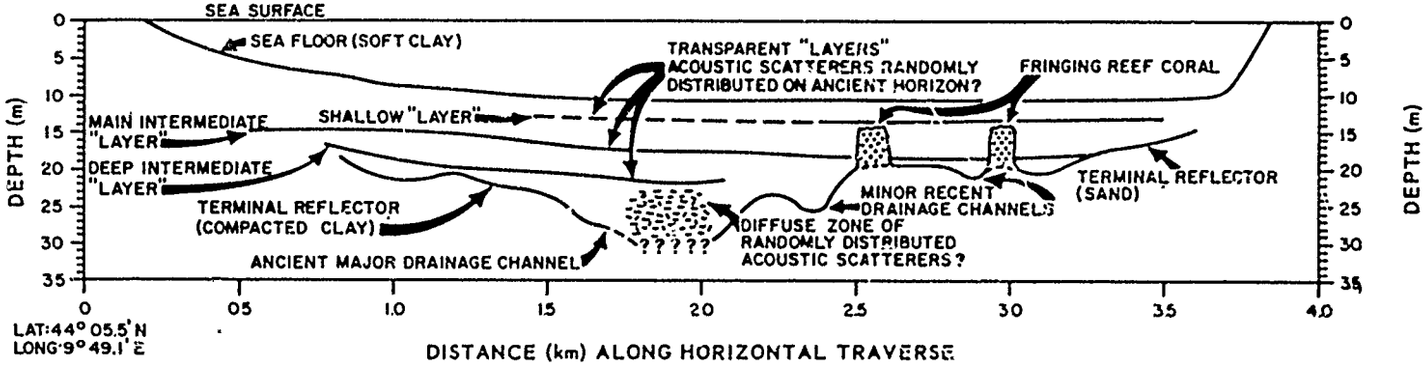

DIAGONAL (NW-SE) STANDARD SECTION

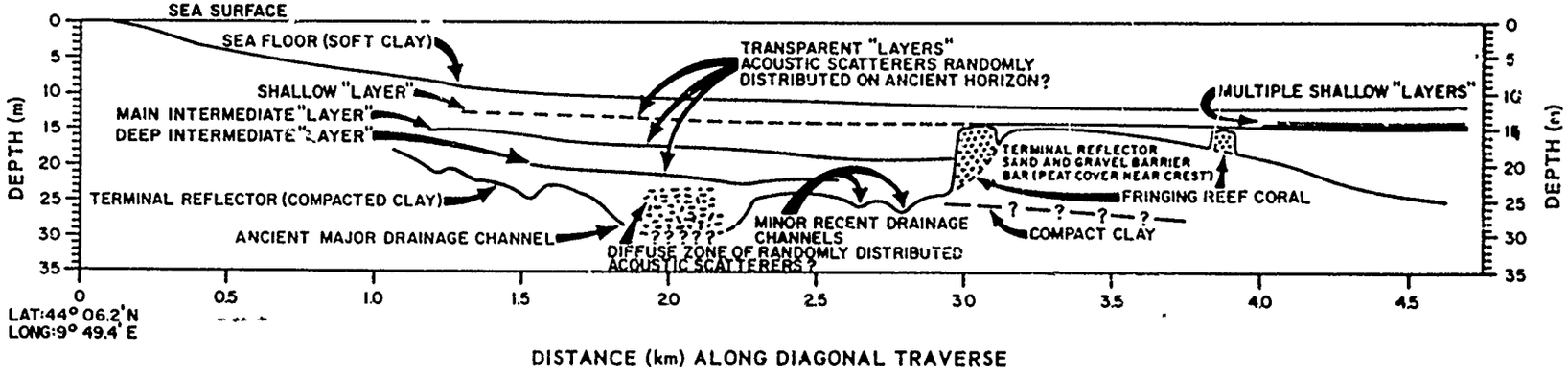

FIG. 24 STANDARD GEOLOGIC SECTIONS IN THE GULF OF LA SPEZIA

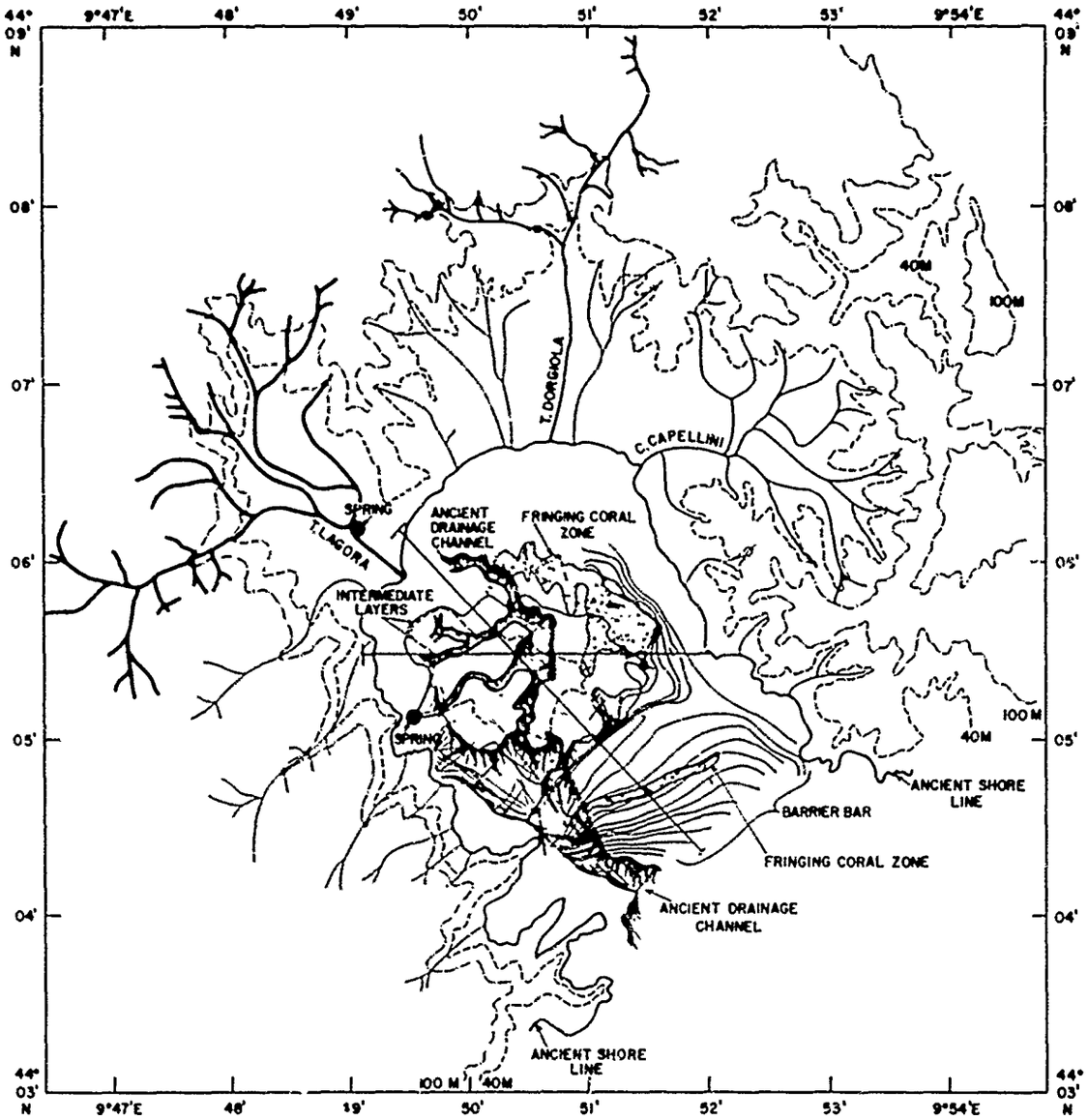

FIG. 25 SUB-BOTTOM GEOLOGY IN THE GULF OF LA SPEZIA

APPENDIX A

TABLE A.1

LOCATIONS OF SEDIMENT CORES AND SURFACE SEDIMENT SAMPLES

SEDIMENT CORE	LATITUDE(N)	LONGITUDE(E)
C1	44°5'06"	9°51'24"
C2	44°4'45"	9°51'50"
C3	44°4'45"	9°51'50"
C4	44°4'41"	9°51'50"
C5	44°4'41"	9°51'50"
C6	44°4'34"	9°52'00"
C7	44°5'06"	9°51'08"
C8	44°5'09"	9°50'51"
C9	44°5'16"	9°50'53"
C10	44°5'19"	9°50'15"
C11	44°5'15"	9°50'13"
C12	44°4'58"	9°50'25"
C13	44°4'52"	9°50'19"
SURFACE SEDIMENT SAMPLE		
S1	44°05'17"	9°51'26"
S2	44°05'12"	9°51'23"
S3	44°05'06"	9°51'55"
S4	44°05'05"	9°52'36"
S5	44°05'38"	9°51'46"
S6	44°04'02"	9°50'33"
S7	44°04'31"	9°50'43"

TABLE A.2

MASS PROPERTIES OF SEDIMENT CORE C-2

Original Distance (m)	Stretched Distance (m)	Water Content (ratio)	Computed Porosity (percent)	Computed Density (g/cm^3)	Sound Velocity (m/sec)	Computed Impedance (10^5 $g/cm^2 \cdot s$)
.05	0.08	1.046	73.6	1.46	1481	2.155
.10	0.15	0.858	69.6	1.52	1477	2.247
.15	0.23	0.805	68.2	1.55	1472	2.274
.20	0.30	0.737	66.3	1.58	1475	2.324
.25	0.38	0.695	65.0	1.60	1474	2.354
.30	0.45	0.681	64.5	1.61	1477	2.371
.35	0.53	0.624	62.5	1.64	1490	2.442
.40	0.60	0.689	64.8	1.60	1473	2.358
.45	0.68	0.690	64.8	1.60	1480	2.368
.50	0.76	0.655	64.0	1.61	1475	2.381
.60	0.91	0.690	64.8	1.60	1469	2.352
.65	0.98	0.673	64.3	1.61	1478	2.378
.70	1.06	0.636	62.9	1.63	1488	2.429
.75	1.13	0.665	64.0	1.61	1487	2.400
.80	1.21	0.644	63.2	1.63	1490	2.424
.85	1.28	0.661	63.8	1.62	1484	2.400
.90	1.36	0.690	64.8	1.60	1491	2.387
.95	1.43	0.617	62.2	1.64	1486	2.442
1.00	1.51	0.602	61.6	1.65	1489	2.463
1.05	1.58	0.649	63.4	1.62	1474	2.393
1.10	1.66	0.633	62.8	1.63	1474	2.409
1.15	1.74	0.614	62.1	1.65	1484	2.442
1.25	1.89	0.607	61.8	1.65	1488	2.456
1.30	1.96	0.612	62.0	1.65	1488	2.451
1.40	2.11	0.543	59.2	1.69	1492	2.527
1.45	2.19	0.608	61.9	1.65	1483	2.444
1.50	2.26	0.604	61.7	1.65	1488	2.457
1.55	2.34	0.612	62.0	1.65	1490	2.453
1.60	2.42	0.582	60.8	1.65	1488	2.481
1.65	2.49	0.600	61.6	1.65	1488	2.460
1.70	2.57	0.606	61.8	1.65	1487	2.454

TABLE A.2 (cont.)

MASS PROPERTIES OF SEDIMENT CORE C-2 (cont.)

Original Distance (m)	Stretched Distance (m)	Water Content (ratio)	Computed Porosity (percent)	Computed Density (g/cm^3)	Sound Velocity (m/sec)	Computed Impedance (10^5 $g/cm^2 \cdot s$)
1.75	2.64	0.638	63.0	1.63	1489	2.429
1.80	2.72	0.616	62.2	1.64	1489	2.448
1.85	2.79	0.589	61.1	1.66	1488	2.473
1.95	2.94	0.610	62.0	1.65	1476	2.431
2.00	3.02	0.586	61.0	1.66	1473	2.450
2.05	3.10	0.588	61.1	1.66	1473	2.448
2.10	3.17	0.597	61.4	1.66	1478	2.449
2.15	3.25	0.584	60.9	1.67	1482	2.467
2.20	3.32	0.591	61.2	1.66	1487	2.453
2.25	3.40	0.599	61.5	1.66	1474	2.439
2.30	3.47	0.603	61.7	1.65	1473	2.433
2.35	3.55	0.596	61.4	1.66	1474	2.442
2.40	3.62	0.604	61.7	1.65	1483	2.450
2.45	3.70	0.606	61.8	1.65	1482	2.447
2.50	3.78	0.589	61.1	1.66	1473	2.448
2.55	3.85	0.560	59.9	1.68	1488	2.502
2.65	4.00	0.568	60.3	1.68	1485	2.487
2.70	4.08	0.562	60.0	1.68	1475	2.479
2.75	4.15	0.578	60.7	1.67	1481	2.471
2.80	4.23	0.585	61.0	1.66	1484	2.469
2.85	4.30	0.597	61.5	1.66	1482	2.452
2.90	4.38	0.562	60.0	1.68	1486	2.497
2.95	4.45	0.566	60.2	1.68	1489	2.497
3.00	4.53	0.570	60.3	1.68	1494	2.502
3.05	4.60	0.561	60.0	1.68	1486	2.496
3.10	4.68	0.562	60.0	1.68	1485	2.495
3.15	4.76	0.554	59.6	1.69	1478	2.493
3.20	4.83	0.567	60.2	1.68	1488	2.495
3.25	4.91	0.536	58.9	1.70	1486	2.523

TABLE A.2 (cont.)

MASS PROPERTIES OF SEDIMENT CORE C-4

Original Distance (m)	Stretched Distance (m)	Water Content (ratio)	Computed Porosity (percent)	Computed Density (g/cm^3)	Sound Velocity (m/sec)	Computed Impedance (10^5 $g/cm^2 \cdot s$)
.05	0.08	1.024	73.2	1.46	1491	2.180
.10	0.17	0.581	60.8	1.67	1486	2.477
.15	0.25	0.731	66,1	1.58	1482	2.340
.20	0.33	0.682	64.6	1.61	1484	2.380
.25	0.42	0.648	63.4	1.62	1488	2.416
.30	0:50	0.664	63.9	1.62	1472	2.378
.35	0.58	0.704	65.3	1.59	1476	2.351
.40	0.67	0.736	66.3	1.58	1477	2.327
.45	0.75	0.771	67.3	1.56	1487	2.320
.55	0.92	0.704	65.3	1.59	1480	2.356
.60	1.00	0.694	65.0	1.60	1476	2.358
.65	1.08	0.652	63.5	1.62	1474	2.391
.70	1.17	0.687	64.7	1.60	1469	2.354
.75	1.25	0.694	64.9	1.60	1466	2.344
.80	1.34	0.678	64.4	1.61	1466	2.356
.85	1.42	0.660	63.8	1.62	1460	2.361
.90	1.50	0.665	64.0	1.61	1456	2.350
.95	1.59	0.658	63.7	1.62	1452	2.350
1.00	1.67	0.643	63.2	1.63	1449	2.357
1.05	1.75	0.660	63.8	1.62	1446	2.339
1.10	1.84	0.635	62.9	1.63	1443	2.355
1.15	1.92	0.605	61.8	1.65	1440	2.376
1.25	2.09	0.629	62.7	1.64	1437	2.350
1.30	2.17	0.686	64.7	1.60	1435	2.300
1.35	2.25	0.628	62.6	1.64	1434	2.348
1.40	2.34	0.635	62.9	1.63	1433	2.339
1.45	2.42	0.600	61.6	1.65	1431	2.367
1.50	2.50	0.600	61.6	1.65	1431	2.366
1.55	2.59	0.641	63.1	1.63	1430	2.329
1.60	2.67	0.673	64.2	1.61	1427	2.299
1.65	2.76	0.660	63.8	1.67	1427	2.307
1.70	2.84	0.653	63.5	1.62	1474	2.391

TABLE A.2 (cont.)

MASS PROPERTIES OF SEDIMENT CORE C-4 (cont.)

Original Distance (m)	Stretched Distance (m)	Water Content (ratio)	Computed Porosity (percent)	Computed Density (g/cm^3)	Sound Velocity (m/sec)	Computed Impedance (10^5 $g/cm^2 \cdot s$)
1.75	2.92	0.617	62.2	1.64	1492	2.452
1.80	3.01	0.649	63.4	1.62	1491	2.420
1.85	3.09	0.631	62.8	1.63	1473	2.406
1.95	3.26	0.641	63.1	1.63	1537	2.504
2.00	3.34	0.650	63.5	1.62	1478	2.398
2.05	3.42	0.654	63.6	1.62	1476	2.391
2.10	3.51	0.712	65.5	1.59	1478	2.349
2.15	3.59	0.647	63.3	1.63	1500	2.438
2.20	3.67	0.639	63.0	1.63	1474	2.404
2.25	3.76	0.636	62.9	1.63	1496	2.441
2.30	3.84	0.623	62.5	1.64	1492	2.445
2.35	3.92	0.613	62.1	1.65	1487	2.446
2.40	4.01	0.630	62.7	1.64	1485	2.428
2.45	4.09	0.641	63.1	1.63	1479	2.408
2.55	4.26	0.605	61.8	1.65	1480	2.442
2.65	4.42	0.610	61.9	1.65	1475	2.432
2.70	4.51	0.636	62.9	1.63	1468	2.396
2.75	4.59	0.681	64.5	1.61	1469	2.359
2.80	4.68	0.631	62.8	1.63	----	-----
2.85	4.76	0.628	62.7	1.64	1458	2.384
2.90	4.84	0.609	61.9	1.65	----	-----
2.95	4.93	0.611	62.0	1.65	1452	2.391
3.00	5.01	0.638	63.0	1.63	1450	2.364
3.05	5.09	0.612	62.0	1.65	----	-----
3.10	5.18	0.602	61.7	1.65	1475	2.437
3.15	5.26	0.613	62.1	1.65	1467	2.414
3.20	5.34	0.631	62.8	1.63	1456	2.379
3.25	5.43	0.578	60.7	1.67	1495	2.494
3.35	5.59	0.615	62.1	1.65	1491	2.453
3.40	5.68	0.614	62.1	1.65	1489	2.450
3.45	5.76	0.621	62.4	1.64	1489	2.442
3.50	5.84	0.602	61.6	1.65	1488	2.461

TABLE A.2 (cont.)

MASS PROPERTIES OF SEDIMENT CORE C-4 (cont.)

Original Distance (m)	Stretched Distance (m)	Water Content (ratio)	Computed Porosity (percent)	Computed Density (g/cm^3)	Sound Velocity (m/sec)	Computed Impedance (10^5 $g/cm^2.s$)
3.55	5.93	0.619	62.3	1.64	1483	2.435
3.60	6.01	0.602	61.6	1.65	1478	2.444
3.65	6.10	0.604	61.7	1.65	1487	2.457
3.70	6.18	0.601	61.6	1.65	1491	2.466
3.75	6.26	0.589	61.1	1.66	1493	2.482
3.80	6.35	0.573	60.5	1.67	1491	2.493
3.85	6.43	0.564	60.1	1.68	1504	2.524
3.90	6.51	0.595	61.4	1.66	1495	2.477
3.95	6.60	0.555	59.7	1.69	1494	2.517

TABLE A.2 (cont.)

MASS PROPERTIES OF SEDIMENT CORE C-11

Original Distance (m)	Stretched Distance (m)	Water Content (ratio)	Computed Porosity (percent)	Computed Density (g/cm^3)	Sound Velocity (m/sec)	Computed Impedance (10^5 $g/cm^2 \cdot s$)
.05	.08	1.330	78.0	1.38	----	-----
.10	.17	1.125	75.0	1.43	1466	2.100
.15	.26	.865	69.8	1.52	1466	2.226
.20	.34	.906	70.8	1.50	1473	2.212
.25	.42	.757	66.9	1.57	1468	2.300
.30	.51	.774	67.4	1.56	1477	2.301
.35	.60	.770	67.3	1.56	1470	2.293
.40	.68	.728	66.0	1.58	1468	2.321
.45	.76	.717	65.7	1.59	1471	2.333
.50	.85	.698	65.1	1.60	1476	2.355
.55	.94	.667	64.0	1.61	1462	2.360
.60	1.02	.685	64.6	1.61	1468	2.355
.70	1.19	.679	64.5	1.61	1467	2.355
.75	1.28	.663	63.9	1.62	1465	2.367
.80	1.36	.641	63.1	1.62	1474	2.402
.85	1.44	.675	64.3	1.61	1468	2.361
.90	1.53	.675	64.3	1.61	1485	2.388
.95	1.62	.744	66.5	1.57	1474	2.319
1.00	1.70	.674	64.3	1.64	1470	2.364
1.05	1.78	.691	64.9	1.60	1471	2.353
1.10	1.87	.705	65.3	1.59	1478	2.354
1.15	1.96	.689	64.9	1.60	1473	2.358
1.20	2.04	.721	65.8	1.59	1467	2.324
1.25	2.12	.680	64.5	1.61	1473	2.365
1.30	2.21	.675	64.3	1.61	1472	2.369
1.40	2.38	.667	64.0	1.61	1473	2.377
1.45	2.46	.672	64.2	1.61	1470	2.368
1.50	2.55	.664	63.9	1.62	1478	2.388
1.55	2.64	.659	63.8	1.62	1472	2.380
1.60	2.72	.659	63.8	1.62	1472	2.381
1.65	2.80	.657	63.7	1.62	1472	2.383
1.70	2.89	.662	63.9	1.62	1475	2.383

TABLE A.2 (cont.)

MASS PROPERTIES OF SEDIMENT CORE C-11 (cont.)

Original Distance (m)	Stretched Distance (m)	Water Water Content (ratio)	Computed Computed Porosity (percent)	Computed Computed Density (g/cm^3)	Sound Sound Velocity (m/sec)	Computed Computed Impedance (10^5 $g/cm^2 \cdot s$)
1.75	2.98	.660	63.8	1.62	1470	2.378
1.80	3.06	.666	64.0	1.61	1476	2.382
1.85	3.14	.643	63.2	1.63	1486	2.419
1.90	3.23	.668	64.1	1.61	1471	2.372
1.95	3.32	.662	63.9	1.62	1471	2.377
2.00	3.40	.657	63.7	1.62	1474	2.387
2.10	3.57	.654	63.6	1.62	1468	2.379
2.15	3.66	.620	62.3	1.64	1470	2.414
2.20	3.74	.647	63.3	1.63	1499	2.437
2.25	3.82	.646	63.3	1.63	1469	2.388
2.30	3.91	.633	62.8	1.63	1471	2.404
2.35	4.00	.612	62.1	1.65	1473	2.423
2.40	4.08	.636	62.9	1.63	1472	2.402
2.45	4.16	.627	62.6	1.64	1476	2.416
2.50	4.25	.626	62.6	1.64	1470	2.407
2.55	4.34	.639	63.0	1.63	1471	2.398
2.60	4.42	.638	63.0	1.63	1472	2.399
2.65	4.50	.644	63.2	1.63	1470	2.392
2.70	4.59	.655	63.6	1.62	1469	2.381
2.80	4.76	.649	63.4	1.62	1466	2.381
2.85	4.84	.636	62.9	1.63	1485	2.424
2.90	4.93	.637	63.0	1.63	1469	2.395
2.95	5.02	.637	63.0	1.63	1466	2.391
3.00	5.10	.631	62.8	1.63	1470	2.401
3.05	5.18	.618	62.3	1.64	1471	2.415
3.10	5.27	.616	62.2	1.64	1468	2.413
3.15	5.36	.612	62.1	1.65	1468	2.415
3.20	5.44	.601	61.6	1.65	1467	2.425
3.25	5.52	.610	62.0	1.65	1486	2.448
3.30	5.61	.617	62.2	1.64	1468	2.414
3.35	5.70	.607	61.8	1.65	1474	2.433
3.40	5.78	.602	61.6	1.65	1473	2.436

TABLE A.2 (cont.)

MASS PROPERTIES OF SEDIMENT CORE C-11 (cont.)

Original Distance (m)	Stretched Distance (m)	Water Content (ratio)	Computed Porosity (percent)	Computed Density (g/cm^3)	Sound Velocity (m/sec)	Computed Impedance (10^5 $g/cm^2.s$)
3.50	5.95	.602	61.6	1.65	1464	2.421
3.55	6.04	.603	61.7	1.65	1474	2.436
3.60	6.12	.604	61.7	1.65	1473	2.434
3.65	6.20	.612	62.0	1.65	1470	2.421
3.70	6.29	.644	63.2	1.63	1465	2.384
3.75	6.38	.601	61.6	1.65	1468	2.428
3.80	6.46	.601	61.6	1.65	1467	2.426
3.85	6.54	.623	62.4	1.64	1467	2.407
3.90	6.63	.624	62.5	1.64	1469	2.408
4.00	6.80	.588	61.1	1.66	1487	2.471
4.05	6.88	.596	61.4	1.66	1475	2.444
4.10	6.97	.578	60.7	1.67	1476	2.463

TABLE A.2 (cont.)

MASS PROPERTIES OF SEDIMENT CORE C-1

Original Distance (m)	Stretched Distance (m)	Water Content (ratio)	Computed Porosity (percent)	Mean Computed Porosity	Density (g/cm^3)	Mean Density (g/cm^3)
0.5	0.7	.706	65.3	65.4	1.59	1.59
		.714	65.6		1.59	
1.0	1.40	.701	65.2	65.9	1.59	1.60
		.683	64.6		1.61	
1.5	2.10	.640	63.1	63.4	1.63	1.62
		.659	63.8		1.62	

TABLE A.2 (cont.)

MASS PROPERTIES OF SEDIMENT CORE C-3

Original Distance (m)	Stretched Distance (m)	Water Content (ratio)	Computed Porosity (percent)	Mean Computed Porosity	Density (g/cm^3)	Mean Density (g/cm^3)
0.5	0.9	0.639	63.0	63.1	1.63	1.63
		.643	63.2		1.63	
1.0	1.74	.641	63.1	63.0	1.63	1.63
		.639	63.0		1.63	
1.5	2.61	.641	63.1	63.0	1.63	1.63
		.636	62.9		1.63	
2.0	3.48	.639	63.1	62.9	1.63	1.64
		.627	62.6		1.64	
2.5	4.35	.609	61.9	61.7	1.65	1.65
		.602	61.6		1.65	
3.0	5.22	.585	61.0	60.8	1.67	1.67
		.577	60.6		1.67	

TABLE A.2 (cont.)

MASS PROPERTIES OF SEDIMENT CORE C-3

Original Distance (m)	Stretched Distance (m)	Water Content (ratio)	Computed Porosity (percent)	Mean Computed Porosity	Density (g/cm^3)	Mean Density (g/cm^3)
0.5	0.9	0.639	63.0	63.1	1.63	1.63
		.643	63.2		1.63	
1.0	1.74	.641	63.1	63.0	1.63	1.63
		.639	63.0		1.63	
1.5	2.61	.641	63.1	63.0	1.63	1.63
		.636	62.9		1.63	
2.0	3.48	.639	63.1	62.9	1.63	1.64
		.627	62.6		1.64	
2.5	4.35	.609	61.9	61.7	1.65	1.65
		.602	61.6		1.65	
3.0	5.22	.585	61.0	60.8	1.67	1.67
		.577	60.6		1.67	

TABLE A.2 (cont.)

MASS PROPERTIES OF SEDIMENT CORE C-8

Original Distance (m)	Stretched Distance (m)	Water Content (ratio)	Computed Porosity (percent)	Density (g/cm^3)
.10	0.12	.958	71.9	1.48
.20	0.24	1.073	74.1	1.45
.30	0.36	.752	66.8	1.57
.40	0.48	.734	66.2	1.58
.50	0.60	.694	65.0	1.60
.60	0.72	.689	64.8	1.60
.70	0.84	.707	65.4	1.59
.80	0.96	.719	65.8	1.59
.90	0.108	.691	64.9	1.60
1.00	1.20	.707	65.4	1.59
1.10	1.32	.699	65.1	1.60
1.20	1.44	.684	64.6	1.61
1.30	1.56	.670	64.1	1.61
1.50	1.80	.669	64.1	1.61
1.60	1.92	.666	64.0	1.61
1.70	2.04	.694	65.0	1.60
1.80	2.16	.665	64.0	1.61
1.90	2.28	.683	64.6	1.61
2.00	2.40	.655	63.6	1.62
2.10	2.52	.650	63.5	1.62
2.20	2.64	.651	64.0	1.61
2.30	2.76	.586	61.0	1.66
2.40	2.88	.697	65.1	1.60
2.50	3.00			
2.60	3.12	.634	62.9	1.63
2.70	3.24	.596	61.4	1.66
2.80	3.36	.614	62.1	1.65
2.90	3.48	.618	62.3	1.64
3.00	3.60	.624	62.9	1.63
3.10	3.72	.632	62.8	1.63
3.20	3.84	.638	63.0	1.63

TABLE A.2 (cont.)

MASS PROPERTIES OF SEDIMENT CORE C-8 (cont.)

Original Distance (m)	Stretched Distance (m)	Water Content (ratio)	Computed Porosity (percent)	Density (g/cm^3)
3.30	3.96	.757	67.0	1.57
3.40	4.08	.638	63.0	1.63
3.50	4.20	.611	62.0	1.65
3.60	4.32	.596	61.4	1.66
3.70	4.44	.601	61.6	1.65
3.80	4.56	.607	61.8	1.65
3.90	4.68	.598	61.5	1.66
4.00	4.80	.592	61.3	1.66
4.10	4.92	.614	62.1	1.65
4.20	5.04	.587	61.0	1.66
4.30	5.16	.614	62.1	1.65
4.40	5.28	.615	62.1	1.65
4.50	5.40	.580	60.8	1.67
4.60	5.52	.542	59.1	1.69

TABLE A.2 (cont.)

MASS PROPERTIES OF SEDIMENT CORE C-10

Original Distance (m)	Stretched Distance (m)	Water Content (ratio)	Computed Porosity (percent)	Mean Computed Porosity	Density (g/cm^3)	Mean Density (g/cm^3)
0.5	0.6	0.781	67.6	66.0	1.55	1.59
		.631	64.5		1.61	
1.0	1.30	.719	65.7	65.8	1.59	1.58
		.724	65.9		1.58	
1.5	1.95	.688	64.7	64.7	1.60	1.60
		.686	64.7		1.60	
2.0	2.60	.718	65.7	65.3	1.59	1.60
		.693	64.9		1.60	
2.5	3.25	.695	65.0	64.8	1.60	1.60
		.684	64.6		1.61	
3.0	3.90	.688	64.8	65.0	1.60	1.60
		.706	65.3		1.59	
3.5	4.55	.694	65.0	64.7	1.60	1.60
		.677	64.4		1.61	
4.0	5.20	.655	63.6	63.5	1.62	1.62
		.650	63.4		1.62	
4.5	5.85	.664	63.9	63.7	1.62	1.62
		.654	63.6		1.62	

TABLE A.2 (cont.)

MASS PROPERTIES OF SEDIMENT CORE C-12

Original Distance (m)	Stretched Distance (m)	Water Content (ratio)	Computed Porosity (percent)	Mean Computed Porosity	Density (g/cm^3)	Mean Density (g/cm^3)
0.5	0.6	1.200	76.2	76.0	1.41	1.42
		1.174	75.8		1.42	
1.0	1.30	.712	65.5	65.1	1.59	1.60
		.690	64.8		1.60	
1.5	1.96	.692	64.9	65.0	1.60	1.60
		.698	65.1		1.60	
2.0	2.62	.669	64.1	64.0	1.61	1.61
		.666	64.0		1.61	
2.5	3.28	.666	64.0	63.8	1.61	1.62
		.657	63.7		1.62	
3.0	3.93	.644	63.2	63.0	1.63	1.63
		.636	62.9		1.63	
3.5	4.58	.614	62.1	62.3	1.65	1.64
		.625	62.5		1.64	
4.0	5.24	.613	63.2	63.0	1.63	1.64
		.631	62.7		1.64	
4.5	5.90	.617	62.2	62.2	1.64	1.64
		.617	62.2		1.64	
5.0	6.55	.610	62.0	62.2	1.65	1.64
		.619	62.3		1.64	

TABLE A.2 (cont.)

MASS PROPERTIES OF SEDIMENT CORE C-13

Original Distance (m)	Stretched Distance (m)	Water Content (ratio)	Computed Porosity (percent)	Mean Computed Porosity	Density (g/cm^3)	Mean Density (g/cm^3)
4.	4.24	.694	65.0	64.8	1.60	1.60
		.687	64.7		1.60	
4.5	4.81	.685	64.7	62.4	1.60	1.60
		.671	64.2		1.61	
5.	5.34	.673	64.2	64.2	1.61	1.61
		.668	64.1		1.61	
5.5	5.88	.656	63.7	63.6	1.62	1.62
		.653	63.6		1.62	
6.	6.42	.634	62.9	62.9	1.63	1.63
		.634	62.9		1.63	
6.5	6.95	.597	61.4	61.4	1.66	1.66
		.595	61.4		1.66	
7.	7.48	.609	61.9	61.8	1.65	1.65
		.606	61.8		1.65	
7.5	8.02	.618	62.2	62.4	1.64	1.64
		.626	62.6		1.64	

(Top 3.5 m of Sediment Core Lost)

TABLE A.3

LOCATION OF SEDIMENT BORINGS

SEDIMENT BORING	LATITUDE (N)	LONGITUDE (E)
D1	44°04'39"	09°50'17"
D2	44°04'59.5"	09°49'26.5"
D3	44°06'03.5"	09°49'06"
D4	44°06'12.5"	09°50'26"
D5	44°06'11"	09°51'17.5"
D6	44°05'11"	09°51'58"

TABLE A.4

RESULTS OF SEDIMENT BORINGS

Borehole D2: This represents 6 boreholes taken within a 50 m zone in the Bay of Cadimare. These boreholes show approximately 16 m of loose clay overlying compacted clay (argilla compatta). In one case seaweed (alghe) and in another case decaying seaweed (alghe in putrefazione) were noted in the loose clay. (Private Communication, Ing. Guiliani, Comune della La Spezia).

Borehole D3: This shows sand, mud and sand with gravel layers overlying the compacted clay interface at 15 m. (Ref. 13).

Borehole D4: This represents 6 boreholes taken within a 200 m zone. These boreholes show loose clay overlying the compacted clay interface at 16 m. (Private Communication, Ing. Prencipe, Shell Oil Co., Istituto di Costruzioni Marittime, Centro Geotechnico Veneto, Università di Padova).

Borehole D5: This represents two boreholes taken within a 50 m zone. They show loose clay overlying a sand and gravel interface at about 12 m. (Private Communication, Ing. Grassi, Cantiere ENEL, Sondaggio No. 29 and No. 30).

Borehole D6: This shows sand, and clay and sand layers interfacing with a layer of rounded cobbles at 30 m. (Private Communication, Ten.Col. Basilio Formisano, MARIGENIMIL, La Spezia).